"Synthesis of thiophosphoramide and phosphoramide ligands and reactivity studies with metal ions"

A Thesis submitted to

Indian Institute of Science Education and Research Pune

in partial fulfillment of the requirements for the

BS-MS Dual Degree Programme

By

Indra Kumar Mahawar
Reg No. 20091022

Thesis Supervisor

Dr. R. Boomi Shankar

Department of Chemistry

Indian Institute of Science Education and Research Pune

Pashan, Pune India 411008

April, 2014

Certificate

This is to certify that this dissertation entitled "Synthesis of thiophosphoramide and phosphoramide ligands and reactivity studies with metal ions" towards the partial fulfillment of the BS-MS dual degree programme at the Indian Institute of Science Education and Research, Pune represents original research carried out by Indra Kumar Mahawar at IISER Pune under the supervision of Dr. R. Boomi Shankar, Assistant Professor, Department of Chemistry during the academic year 2013-2014.

Signature of student:

Date: 2/4/2014

Place: Pune

Signature of supervisor
(Dr. R. Boomi Shankar)

Date: 2/4/2014

Place: Pune

Declaration

I hereby declare that the matter embodied in the report entitled "Synthesis of thiophosphoramide and phosphoramide ligands and reactivity studies with metal ions" are the results of the investigations carried out by me at the Department of Chemistry, IISER Pune, under the supervision of Dr. R. Boomi Shankar and the same has not been submitted elsewhere for any other degree.

Date: 2/4/2014 Mr. Indra Kumar Mahawar

Place: Pune ID: 20091022

Acknowledgment

First of all I would like to offer my special thanks to Dr. R. Boomi Shankar who gave me this wonderful opportunity to carry out this research work and also for his constant help and encouragement. He is a good human being and perfect team leader. I would like to acknowledge the help provided by Dr. V.G. Anand. This project would not have been completed without the help of several people. Anant Kumar Srivastava (PhD student) comes on the first position in the list of my co-guides/colleagues. He is very helpful and active person. He helped me to learn sufficient technique during my research project. I can not forget other members of my group who helped me on every single day. I was benefited by Arvind, Ashok and Mahesh's lab experience. I am grateful to work with my colleagues Arun, Vijaykant, Rajshekhar, Rajkumar, Vimlesh, Rupal who made friendly environment for research work. I am also grateful to the technical staff and non-technical staff of IISER-Pune. I am extremely grateful to my parents and brothers for supporting and encouraging me every moment. I am also very thankful to all my friends of 2009 batch for making IISER-Pune life enjoyable.

Table of Contents:

Abbreviations:

Anal.	Analysis
ESI	Electron spray ionization
IR	Infrared spectroscopy
UV	Ultraviolet
NMR	Nuclear magnetic resonance
MALDI –TOF	Matrix-Assisted laser desorption/ionization-time of flight
Py	Pyridyl
Ph	Phenyl
^{i}Pr	Isopropyl
NPs	Nano particles
FPs	Fine particles
^{t}Bu	Tert-butyl
SC-XRD	Single crystal X-ray diffraction
PXRD	Powder X ray diffraction
O_{water}	Oxygen atom of water
$N_{pyridyl}$	Nitrogen atom of pyridyl
MeOH	Methanol
Equiv.	Equivalent
TBN	Tetrabutyl ammonium nitrate
L	2-pyridyl (py)-functionalized phosphoric triamide
L^1	Tris(iso-propyl) thiophosphoramide
L^2	Bis(3-Pyridyl) t-butyl phosphoramide
ml	Milliliter
µl	Microliter
°C	Degree centigrade
mp	Melting point

List of figures:

ABSTRACT

Various phoshoramide and thiophosphoramide ligands containing hard and soft donor functionalities were synthesized and their reactivity studies were carried out with various transition metal ions. Using tris(alkylamido) functionalized thiophosphoramide ligands, interesting examples of Ag(I), Cd(II) and Pd(II) complexes were synthesized. Further, some of these complexes were used as single-source precursors for stabilizing the corresponding metal-sulfide nano-particles such as Ag_2S and CdS nano-particles. These nano-particles were found to be stabilized by the thio-functionalities of the phosphoramide ligands. In another related system using the t-butyl phosphoric diamide ligand containing 3-pyridyl functionalities, interesting examples of metal complexes were obtained as discrete and polymeric assemblies. The Cu(II) complexes of this ligand were obtained as 1D- and 2D-polymeric complexes depending upon the counter ions, While a discrete trinuclear macrocyclic structure cage was obtained for the Ni(II) ions.

Introduction

Phosphorous is one of the important elements in main group of the periodic table and finds utility in all the areas of chemistry, from organic chemistry to material chemistry through inorganic chemistry, organometallic chemistry and bio-inorganic chemistry. Phosphorus-nitrogen compounds are a major family of phosphorus containing compounds which has been explored extensively in the past five decades or so (Figure 1).[1] Among these, Imino derivatives of P(V) compounds are one of the simplest class of compounds that are utilized in coordination chemistry because of their ability to act as the N-analogues of common phosphorus oxo anions (Figure 2).[2] Several research groups including that of ours are working on the coordination chemistry of imido P(V) anions. Metal complexes of several P(V)-imido anions were utilized as catalytic systems for olefin oligomerization[3] and polymerization,[4] ring-opening polymerization of lactides,[5] hydroamination[6] and transfer hydrogenation[7] etc. Some of these metal complexes have also shown to form long lived paramagnetic radicals upon oxidation.[8]

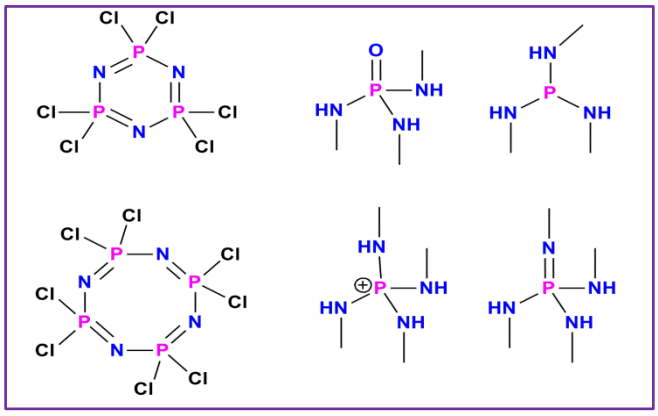

Figure 1: Some examples of Phosphorous containing compound.

The first example of an imido-phosphate trianion as its lithium complex was reported by Steiner, Wright and co-workers in the reaction involving diphosphrous tetraiodide and α-naphthylamine in presence of n-BuLi.[9] Subsequently, it was shown that tetra(anilino)phosphonium chloride, $[P(NHPh)_4]Cl$, can be sequentially deprotonated to generate the homoleptic imido moieties analogues to H_3PO_4, $H_2PO_4^-$, HPO_4^{2-} and PO_4^{3-} ions, respectively.[10] Chivers and coworkers have synthesized metal complexes of several homo- and heteroleptic imido-phosphate derivatives of the type $[(RN)_{3-x}(RNH)_xP=E]^{x-3}$ (E = $NSiMe_3$, O, S or Se and X = 0, 1 or 2) using the highly reactive organometallic bases (M)

such as RLi, R_2Zn, R_2Mg and R_3Al (R is any alkyl or aryl group). Although these imido-P(V) anions are ubiquitous in the reactions involving amido-phosphate ligands and organometal alkyls/aryls/silylimides in non-polar medium, their stability in aprotic and polar solvents have been very poor. This is particularly attributed to the highly reactive nature of the metal ions employed as well as to the presence of residual metal-alkyl/aryl/silyamide bonds in these complexes. It has also been noticed that use of Lewis acidic transition metal ions in these deprotonation reactions has lead to the cleavage of P-N bonds instead of the N-H bond activation.[11] Prompted by these observations, our group has been looking at using certain reactive metal salts as a source of base to generate the P(V) bound polyimido species in polar medium.[12]

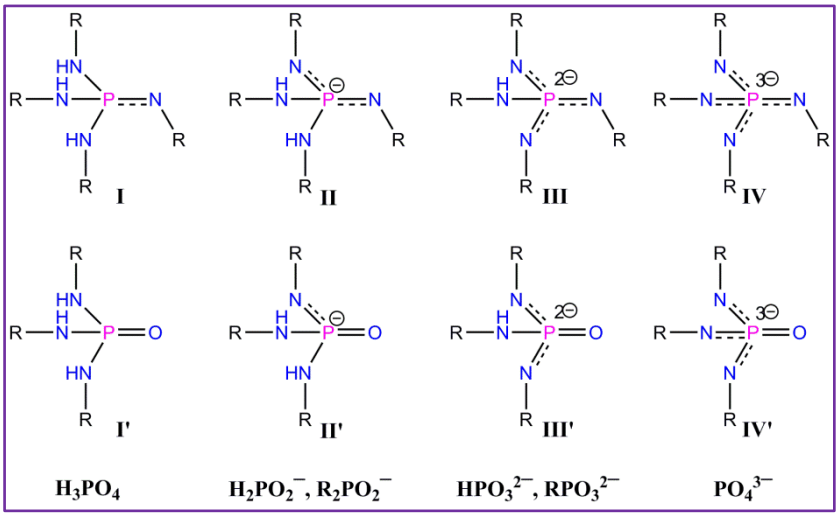

Figure 2: Iso-electronic species.

In this efforts our group has synthesized various known and new amino P(V) compounds and started looking at their properties extensively. In these experiments our group has synthesized several examples of phosphonium cations of the formula $[(RNH)_4P]^+$. These Phosphonium cations, in the presence of chloride, carboxylate and polyoxometalate anions, were used to make designer supramolecular structures aided by hydrogen bonding interactions.[13] The four RNH groups located on the tetra(organoamino)phosphonium cations of formula $[(RNH)_4P]^+$ are arranged in a tetrahedral fashion around the central phosphorus atom (Figure 3). This arrangement of phosphonium cations gives a distinctive geometry for hydrogen bonding which is different from planar N–H donors such as urea and guanidinium motifs.[14]

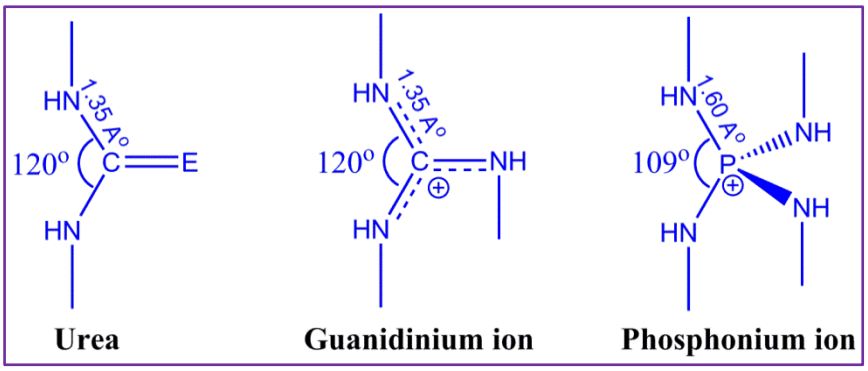

Figure 3: Structural comparison of Phosphonium ion.

Subsequently, to check the deprotonation behaviour, several alkyl or peripherally functionalized amino P(V) compounds were subjected to reactions with various reactive metal salts. Thus, the treatment of tetrakis(2-pyridylamino)phosphonium chloride, $[P(NHpy)_4]Cl$, with $AgClO_4$ have shown to yield a pentanuclear Ag(I) complex (Figure 4) sandwiched between two mono-anionic imido ligands $[P(Npy)_2(NHpy)_2]^-$ of the type II'(Figure 2).[15]

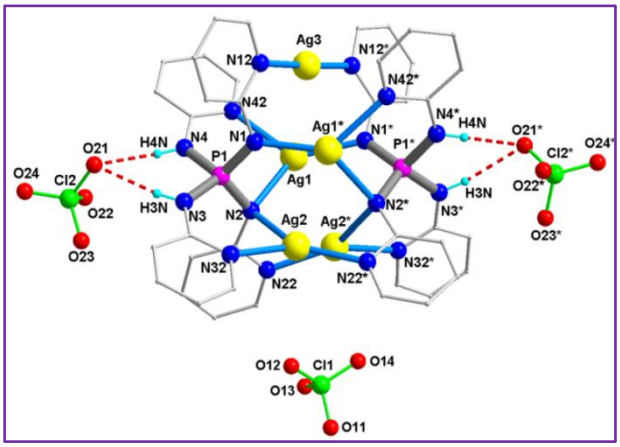

Figure 4: Penta nuclear Ag complex.

Further, it has been shown that the 2-pyridyl (py)-functionalized phosphoric triamide $[PO(NHpy)_3]$ can be subjected to step-wise deprotonation in presence of various silver(I) salts. In view of the versatile coordination a 2-pyridyl (py)-functionalized phosphoric triamide $[PO(NHpy)_3]$ was reacted with $Ag(ClO_4)$ to generate octa nuclear mono-deprotonated $[Ag_8(LH_2)_4]^{4+}$ complex (Figure 5) featuring the mono-anionic ligand of the type II' (Figure 2). When this 2-pyridyl (py)-functionalized phosphoric triamide $[PO(NHpy)_3]$ was treated with $AgBF_4$, di-deprotonated hepta nuclear $[Ag_7(LH)_3]^+$ complex (Figure 5) was

obtained containing the anionic ligand of the type III' (Figure 2). A tri nuclear $[Ag_3(LH_3)_2]^{3+}$ complex (Figure 5) of the neutral ligand, (LH_3), was obtained when $AgNO_3$ was used in this reaction as no ligand deprotonation occurs in this reaction.[12]

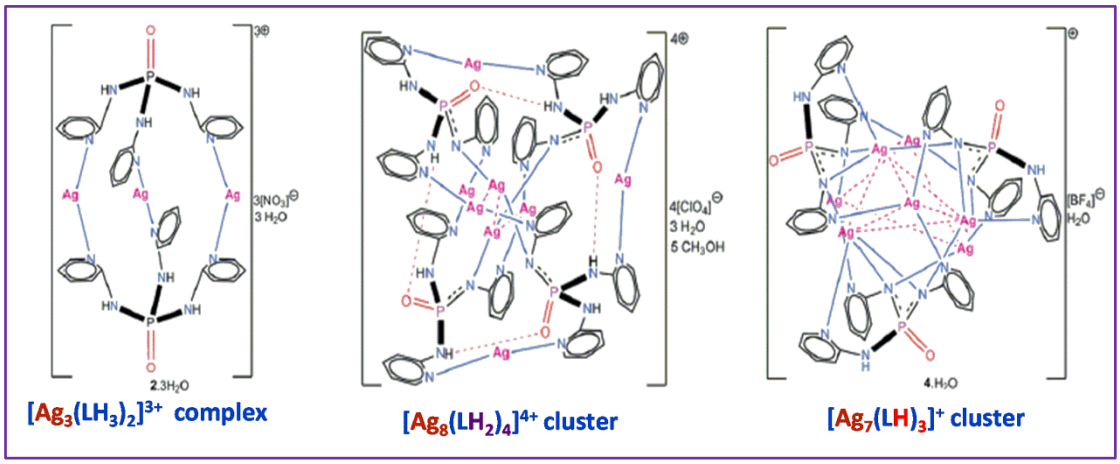

Figure 5: Ag(I) clusters.

Inspired by the remarkable utility of palladium and its compounds in various organic bond-activation reactions,[16] the salts of Pd(II) ions were employed in deprotonation reactions with these amido P(V) ligands. Thus the reaction of $[PO(NHpy)_3]$ with $PdCl_2$ gave rise to a dinuclear complex of formula $\{PdCl[PO(Npy)(NHpy)_2]\}_2$ for the monoanionic ligand of the type II' (Figure 2).[17] In a remarkable discovery fully deprotonated tris(imido)phosphate trianions of the type $[(RN)_3PO]^{3-}$ starting from $[(NHR)_3PO]$ and $Pd(OAc)_2$ were reported in polar solvents such as CH_3OH, CH_3CN, $(CH_3)_2SO$, etc. These highly basic anions were isolated as their corresponding tri- and hexanuclear Pd(II) clusters (Figure 6). All these complexes contain one or two triangular Pd_3 motifs in which the Pd(II) atoms are bound to three chelating N_{imido} moieties.

Nucleophilic reagents such as primary amines $(R''NH_2)$ was reacted at the Pd(II) atoms in the hexameric Pd_6-clusters to generate a trimeric species with the formula $\{Pd_3[(NR)_3PO](OAc)_3(R''NH_2)_3\}$ (Figure 7). These trimeric species were obtained via the symmetrical cleavage of the hexamer. Here the three Pd−Nimido moieties attached to the Pd_3 subunit exhibit good stabily and remain unaffected during the cleavage reaction. Further these Pd(II) complexes were used in Mizoroki−Heck (M−H) type coupling reaction.[18]

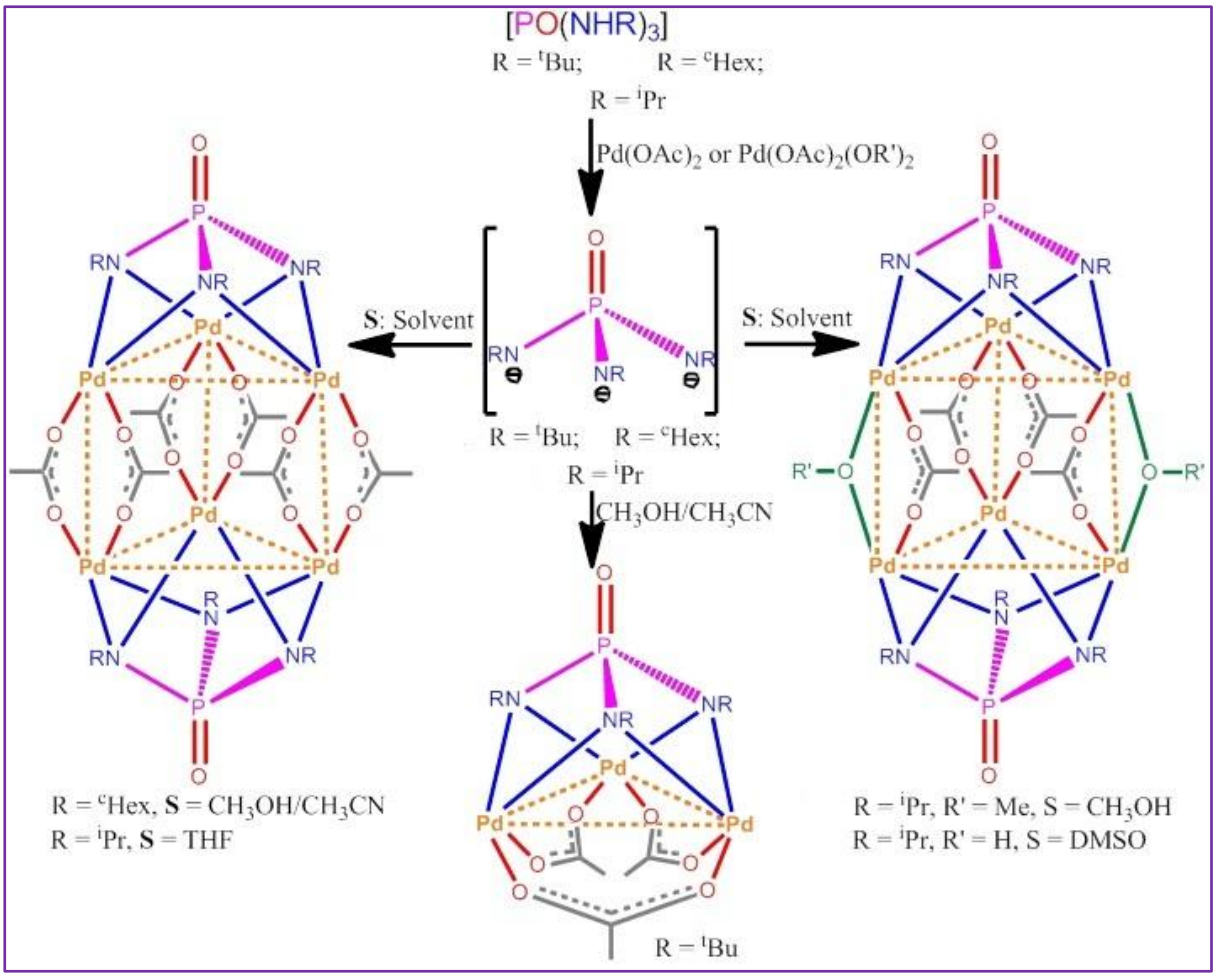

Figure 6: Tri and hexa nuclear Pd(II) clusters.

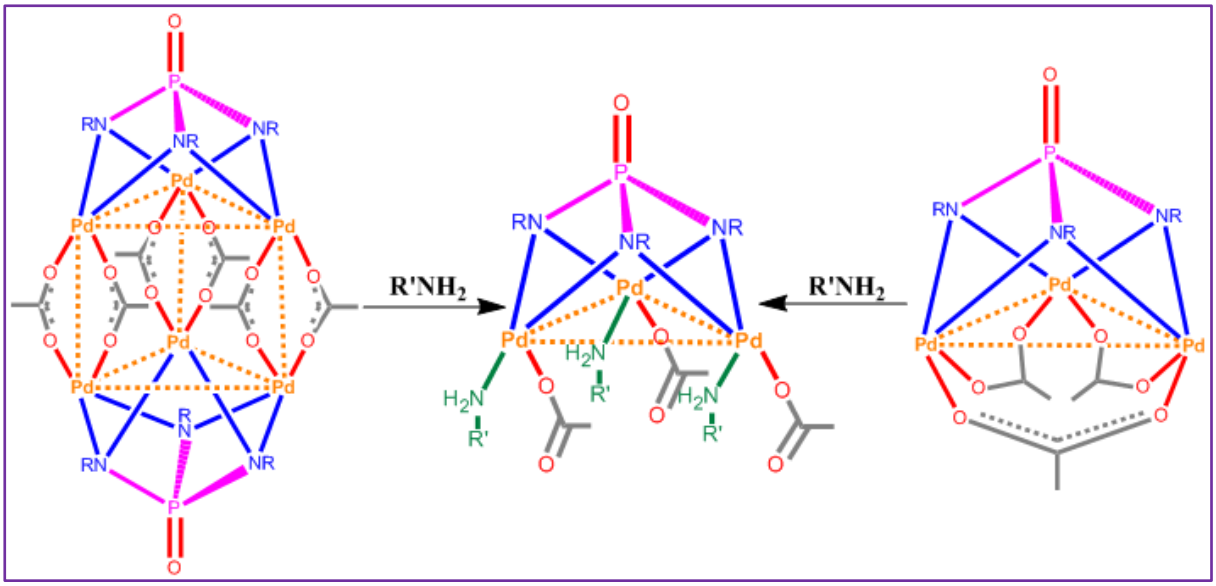

Figure 7: Synthesis of trinuclear Pd(II) cluster.

From these results it is apparent that use of mildly Lewis acidic metal ions in reaction with amino P(V) ligands lead to the formation of the various imido (V) anions. These reactions are further facilitated, in some cases, by the presence of peripheral metal coordinating groups. So far the mild- deprotonation approach is limited only to phosphonium cations and phosphoric triamides. Inspired from these results, we were interested in extending the deprotonation chemistry to other systems viz., tri-functional thiophosphoramides and bi-functional alkyl/aryl phosphoramides. Although, we were able to see the deprotonation in a few instances, several other reactions showed that these ligands were used as neutral ligands for the soft metal ions employed in these reactions. Especially, the thiophosphoramides interact with soft metal ions through its softer sulfur atom leading to simpler molecular architectures. However, these complexes were shown to act as single source precursor for obtaining the corresponding metal sulfide particles. The coordination chemistry of a t-butyl phosphoric diamide ligand containing a 3-pyridyl groups were studied in detail as well.

Results and Discussions

Section I: *Synthesis and Reactivity studies of the tris(iso-propyl) thiophosphoramide, [PS(NH^{i}Pr)$_3$], ligand (**L^1**).*

Synthesis:

The thiophosphoramide **L^1** was synthesized according to the previously reported procedure which involves the reaction of $PSCl_3$ with excess i-propyl amine in refluxing toluene as shown in scheme 1.[19] ^{1}H NMR peaks represent the ligand **L^1** (Figure 8). The ^{31}P-NMR of **L^1** gave a sharp peak at δ 58.56 (lit. 58.6) (Figure 9). The high-resolution ESI-MS spectrum of **L^1** gave a peak at m/z = 238.1507 for the parent ion (Figure 10).

Scheme 1

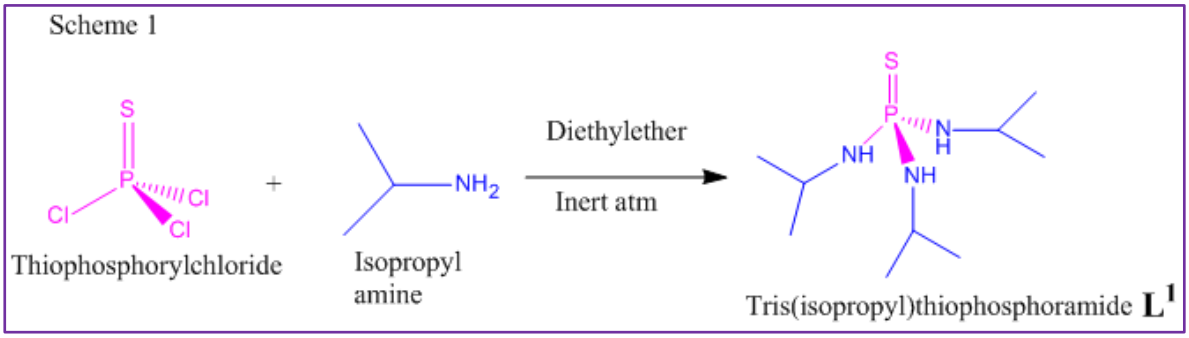

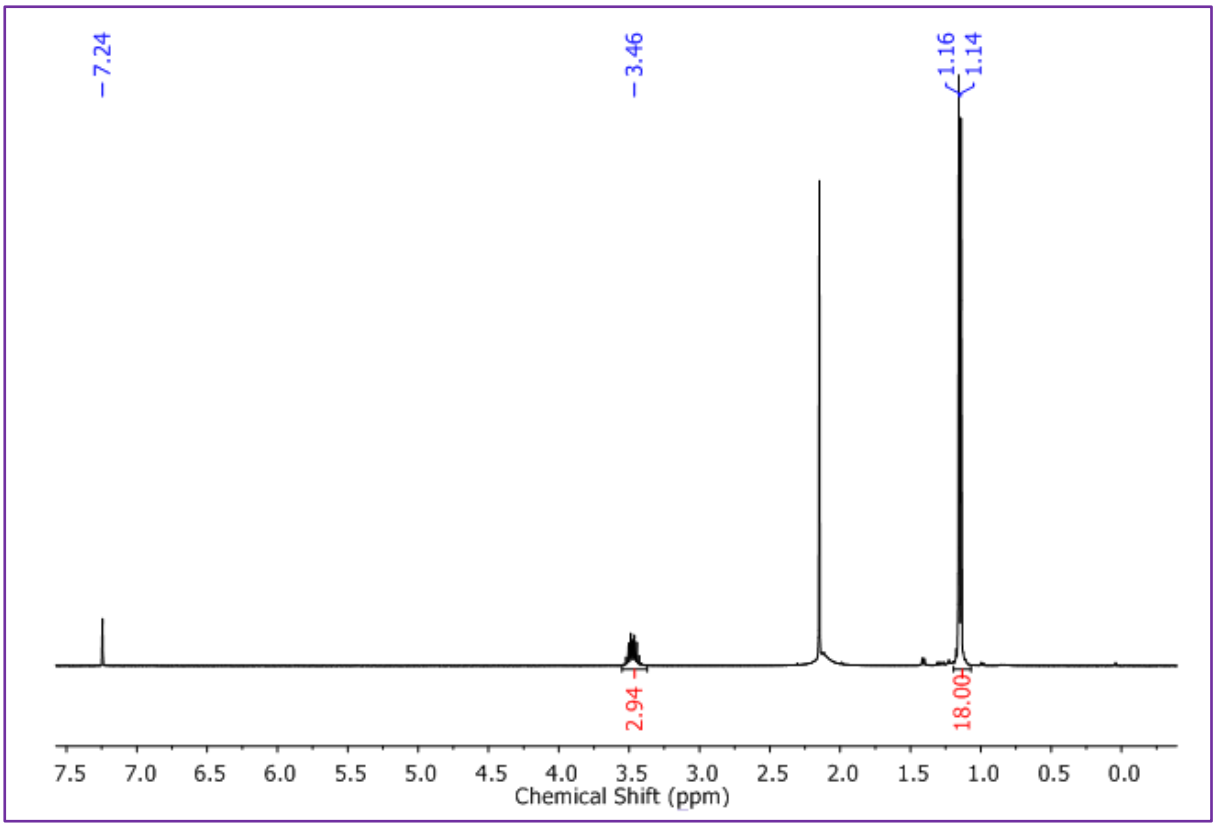

Figure 8: ^{1}H NMR of Tris(isopropyl)thiophosphoramide.

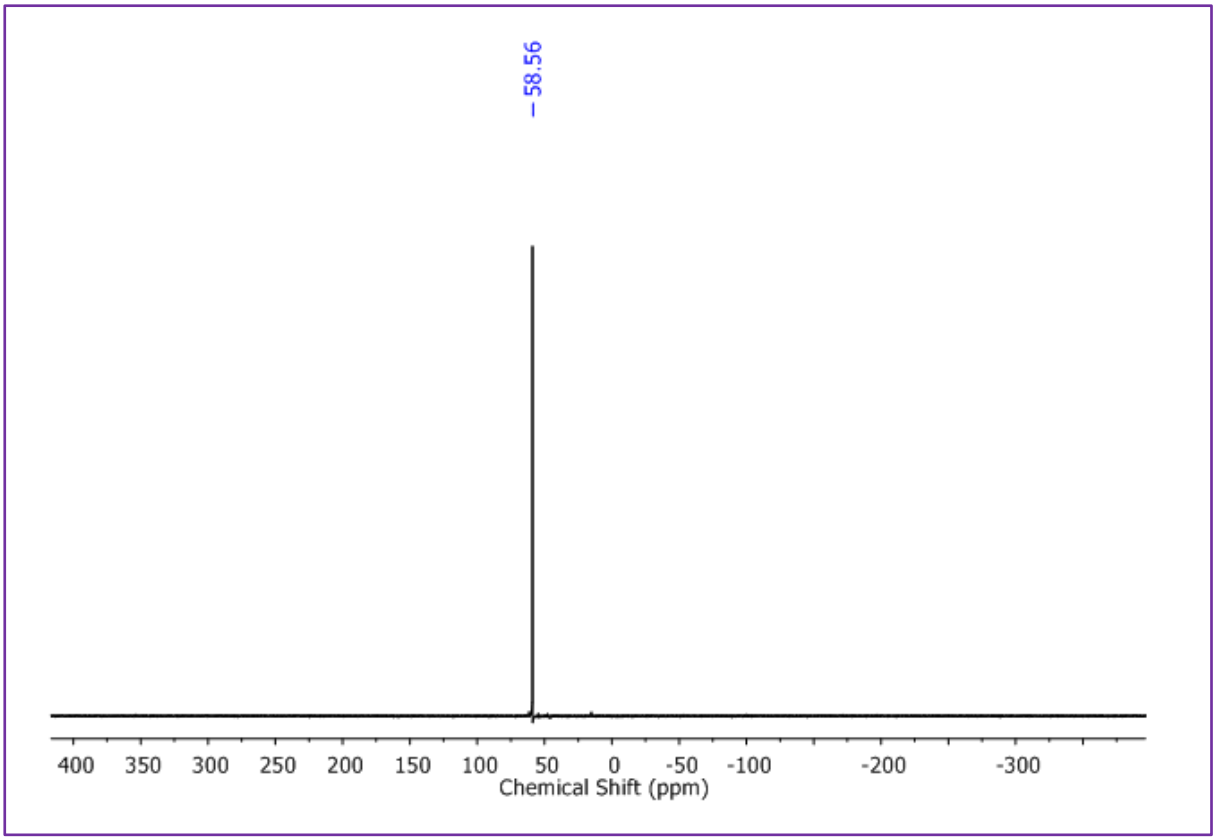

Figure 9: ^{31}P NMR of Tris(isopropyl)thiophosphoramide.

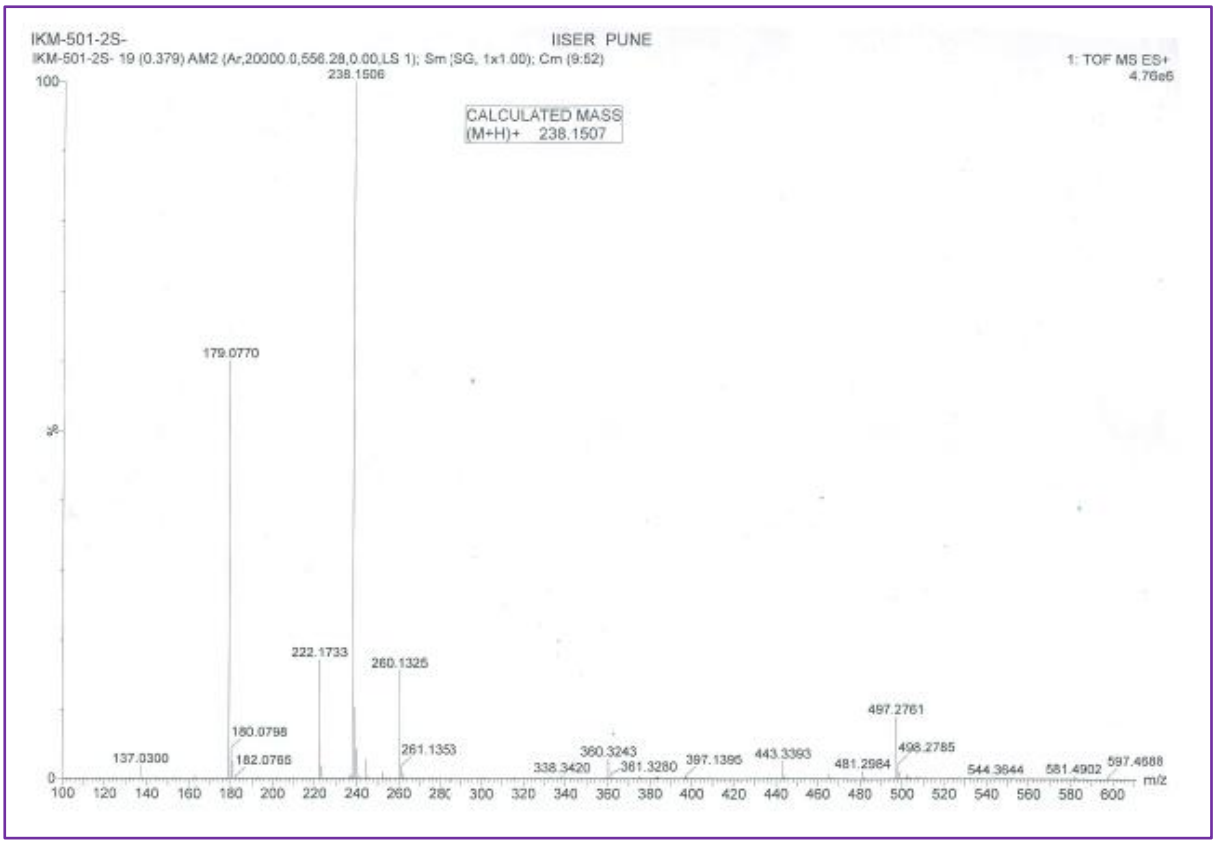

Figure 10: HRMS of Tris(isopropyl)thiophosphoramide.

In order to study the deprotonation chemistry of this ligand, we subjected it to reactions with salts of Pd(II), Ag(I) and Cd(II) ions. The reaction of $\mathbf{L^1}$ with $Pd(OAc)_2$ in methanol proceeded smoothly and gave orange coloured crystals (in low yields) in about 10-15 days. The single crystal X-ray analysis of these crystals revealed the formation of a tri-nuclear palladium sulfide complex of formula $Pd_3S_2[PS(NH^iPr)_3].(OAc)_2$ (**1**) in which no ligand deprotonation was observed. The origin of the sulfide ion can be tracked to the hydrolytic cleavage of the some of the ligands P=S bonds in the polar medium (Figure 13). Due to poor yield of the sample, we were unable to obtain the NMR and mass-spectral data for this complex. In order to improve the yield of the complex **1**, we repeated the reaction in presence of elemental sulfur powder. However, the obtained solids did not match well with the physical properties of the crystalline sample of **1** (melting point and PXRD). Further, in an attempt to deprotonate the ligand amino protons, the reaction was performed in presence of several bases such as KOH, Et_3N and aqueous NH_3. Among these, the reaction involving aqueous NH_3 gave a clean product. The single crystal X-ray analysis has revealed a mono deprotonated species (similar to II') in complex $Pd[PS(N^iPr)(NH^iPr)_2]_2$. The presence of this species in solution was confirmed from MALDI-TOF mass spectrum which gave a *m/z* 580

for the parent ion species (Figure 11(b)). The peak at *m/z* 522 corresponds to the complex fragment where an iso-propylamine arm from one of the ligand in the complex is cleaved (Figure 11(a)).

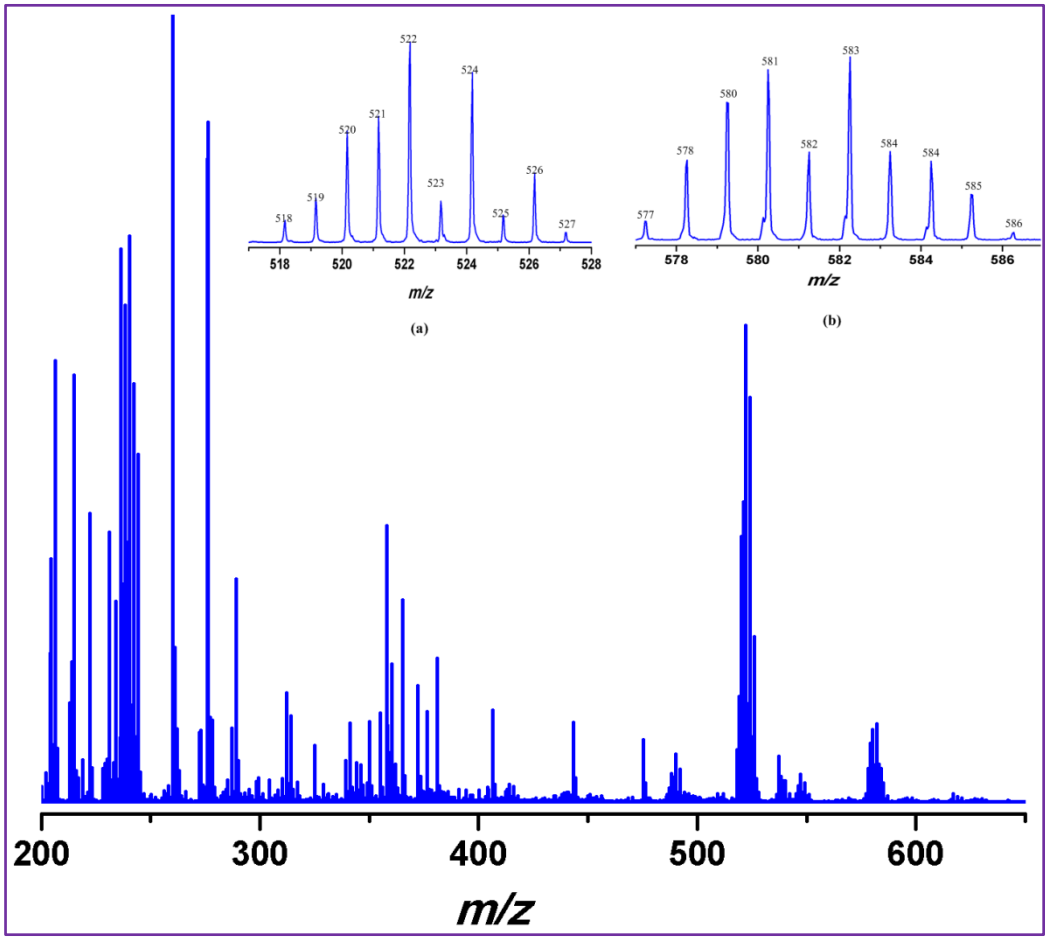

Figure11: MALDI-TOF Mass spectra of **2**: *m/z* 580.

The reaction of $\mathbf{L^1}$ with $Cd(ClO_4)_2$ and $AgNO_3$ gave the respectively the mono-nuclear and 1D-polymeric complexes of formula $Cd[PS(NH^iPr)_3]_4.2ClO_4$ and $\{Ag[PS(NH^iPr)_3].NO_3\}_n$. The single crystal X-ray analysis of these complexes revealed that the metal ions are coordinated from the donor S-atom and no ligand deprotonation. Stability of complex **3** in solution was estimated by MALDI-TOF, where the spectra shows a peak at *m/z* 537 which corresponds to half the total mass of complex **3** (Figure 12).

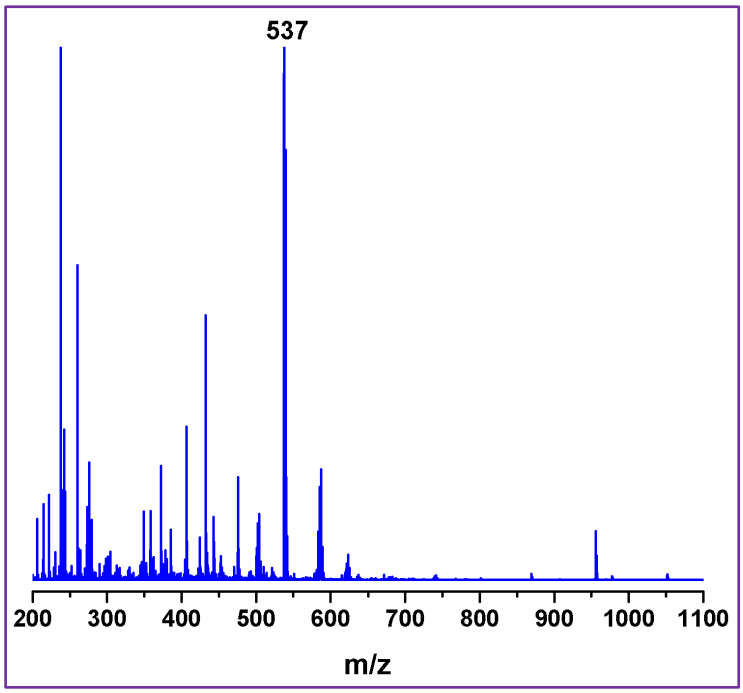

Figure12: MALDI-TOF Mass spectra of **3** $(M/2)^+$: *m/z* 537).

In view of the loosely bound nature of the M-S bonds in these complexes, we explored their utility in obtaining the corresponding metal–sulfide particles.

Crystal Structures:

$Pd_3S_2[PS(NH^iPr)_3].(OAc)_2$ [1]: The trinuclear species **1** was crystallized in the monoclinic space group $P2_1/n$. The molecular core consists of six ligands $\mathbf{L^1}$, three Pd(II) atoms, two sulphide ions and two acetate ions (Figure 13). The Pd(II) centers are connected to each other making a triangular plane, with the two sulphide ions attached to them from both top and bottom side of triangular surface in a capping manner. In addition, each Pd(II) ion is connected to two thiophosphoramide ligands through $S_{phosphoryl}$. The Two uncoordinated acetate anions provide the charge balance in the molecule. The Pd-$S_{phosphoryl}$ distances ranges from 2.373 Å to 2.414 Å. While the Pd-S bond distances for sulfide ions are in the range of 2.302 Å-2.324 Å. No sign of deprotonation of the amido protons by Pd(II) metal ion were observed in this case.

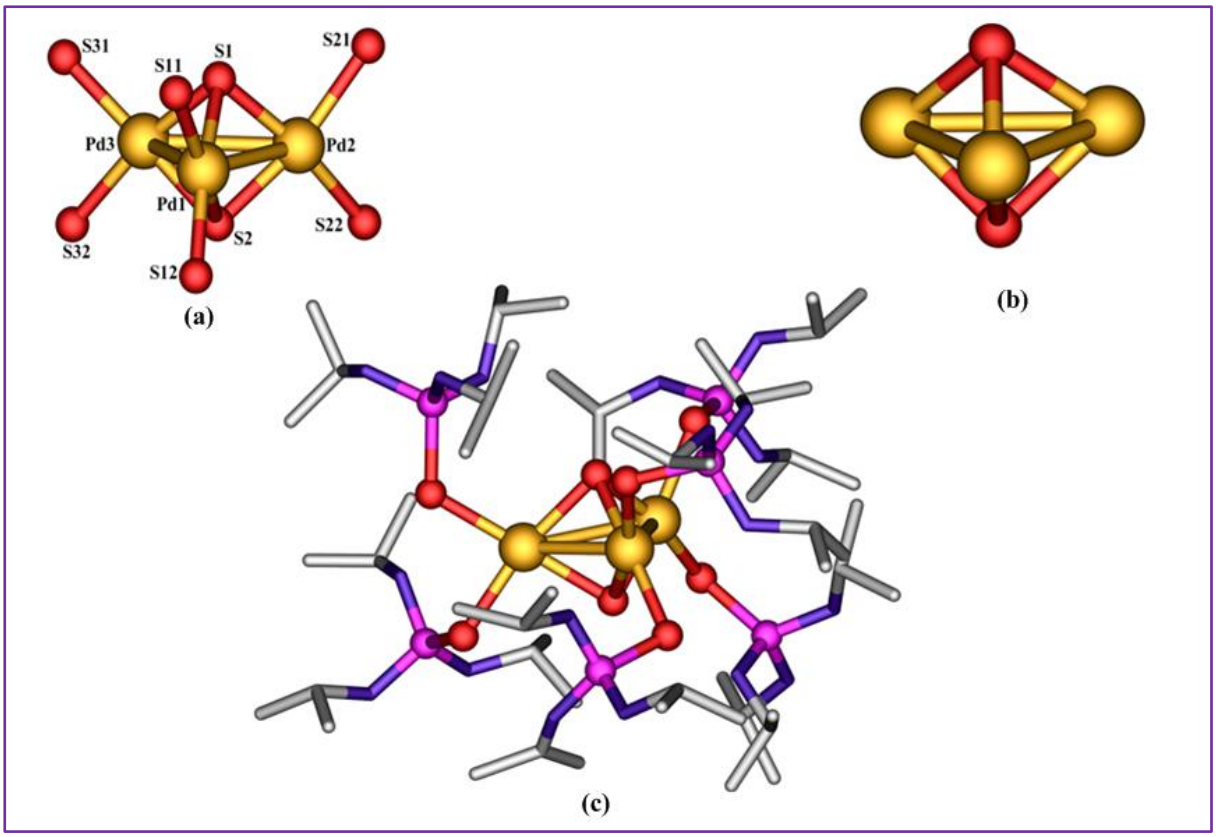

Figure13: (a) The coordination environment of the Pd_3-unit, (b) View of the trigonal bipyramidal Pd_3S_2 cluster; (c) Crystal structure of complex **1.**

$Pd[PS(NH^iPr)_2(N^iPr)]_2$ [2]: The Mononuclear complex **2** was crystallized in the monoclinic crystal system, space group $P2_1/c$. The molecular core consist of a single Pd(II) ion and two $\mathbf{L^1}$ ligands (Figure 14). In complex **2**, both the ligands are monoanionic due to the deprotonation of one of the amido proton. Hence Pd(II) metal ion is bonded to each ligand by N_{imido} and the S atom of the ligand $\mathbf{L^1}$. The Pd -N_{imido} bond distances were in the range of 2.023 Å to 2.046 Å, while the Pd-S distances are found in the range of 2.320 Å - 2.326 Å.

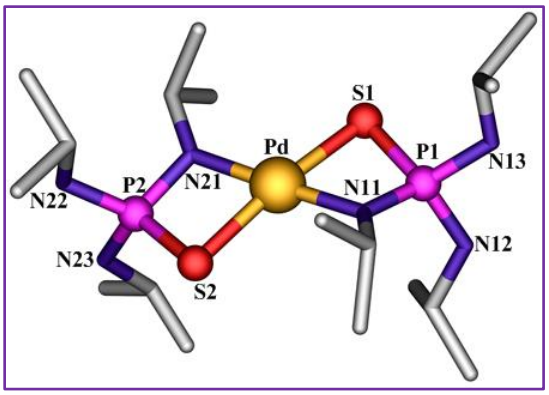

Figure 14: Mono nuclear Pd(II) complex **2** with mono anionic ligand $\mathbf{L^1}$**.**

$Cd[PS(NH^iPr)_3]_4.2ClO_4$ [3]: The complex **3** was crystallized in monoclinic space group $P2_1/c$. The molecular core of **3** consists of one Cd(II) metal ion, four $\mathbf{L^1}$ ligands and two perchlorate anions (Figure 15). Four ligands ($\mathbf{L^1}$) are connected to the Cd(II) center through phosphoryl-S atom in tetrahedral geometry. The Cd-S bond distances were found in the range of 2.529 Å -2.550 Å.

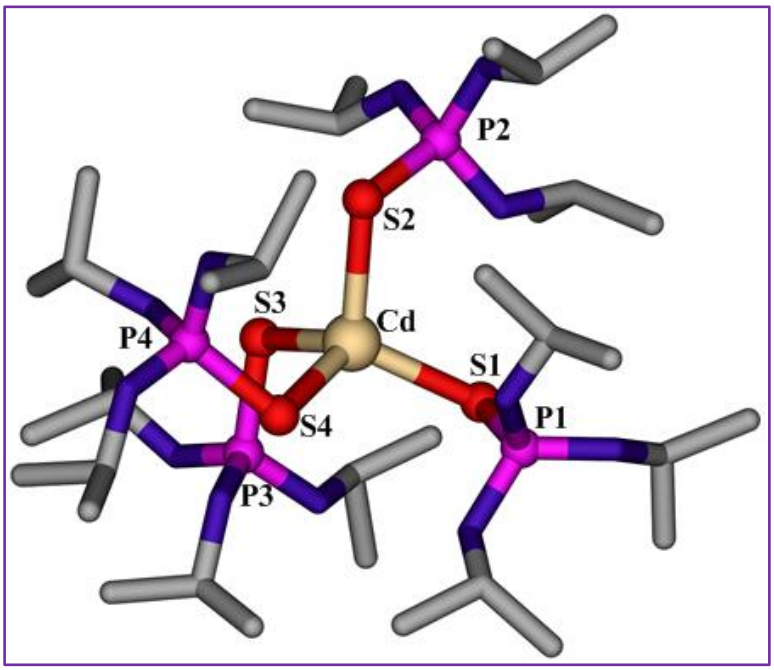

Figure 15: Tetrahedral arrangement of complex **3.**

$Ag[PS(NH^iPr)_3].NO_3$ [4]: The complex **4** was crystallized in the monoclinic space group $P2_1/c$. The asymmetric unit of **4** consists of one silver atom, one $\mathbf{L^1}$ ligand and a nitrate anion (Figure 16). The Ag metal ion is bonded to phosphoryl-S atom of ligand $\mathbf{L^1}$ and oxygen of the nitrate anion. Propagation of the asymmetric unit of complex **4** leads to a 1D chain of Ag-S string. The Ag-S bond distances were found to be in the range of 2.421 Å -2.439 Å, while the Ag-O bond distance was 2.456 Å.

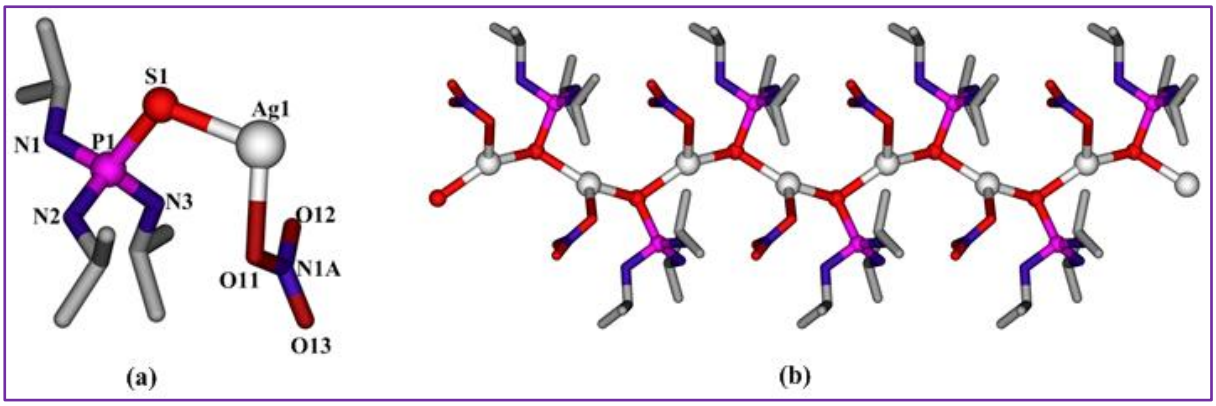

Figure 16: (a) Asymmetric unit and (b) 1D polymeric chain structure of **4**.

TGA and PXRD for compounds 1, 2, 3, 4:-

For checking the thermal stability of the complex **1** and **4**, Thermo Gravimetric Analysis (TGA) was performed over a range of temperatures from 30 °C to 550 °C. The TGA plot given in Figure 17 shows that complex **1** is stable up to 160 °C, after which it shows an abrupt weight loss suggesting its decomposition above 160 °C. The TGA plot in Figure 17 shows the stability of **4** up to 200 °C. Above this temperature an abrupt weight loss was observed indicating the decomposition of the complex **4**.

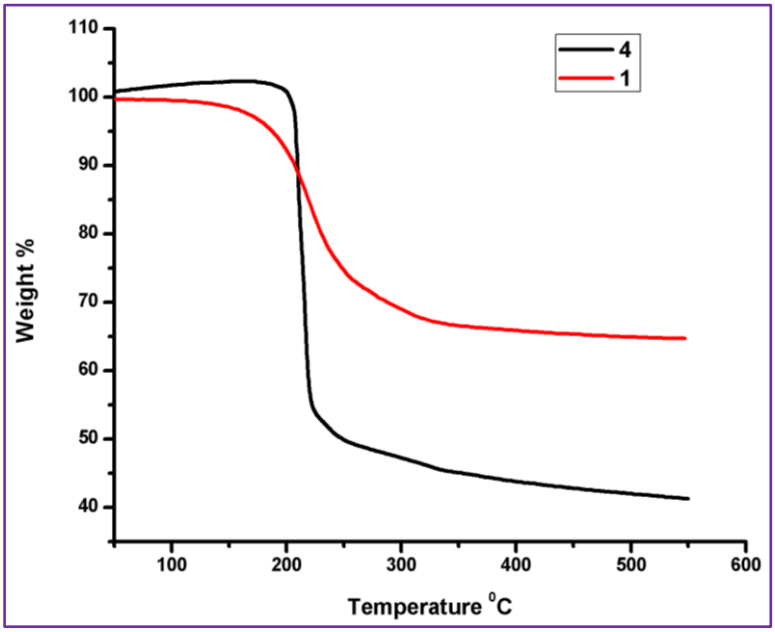

Figure 17: Thermo gravimetric analysis data showing weight loss of complexes **1** and **4**.

Further the phase purity and crystallanity of the synthesized complexes **2, 3** and **4** in powder form was checked using Powder X-Ray Diffractometer (PXRD) at room temperature (Figure 18). As observed from the graph, the PXRD pattern for the as-synthesized complex **3, 4** matches with the simulated pattern obtained from the crystal structure, but the PXRD pattern for complex **2** shows mismatch in intensities mostly at higher 2θ values.

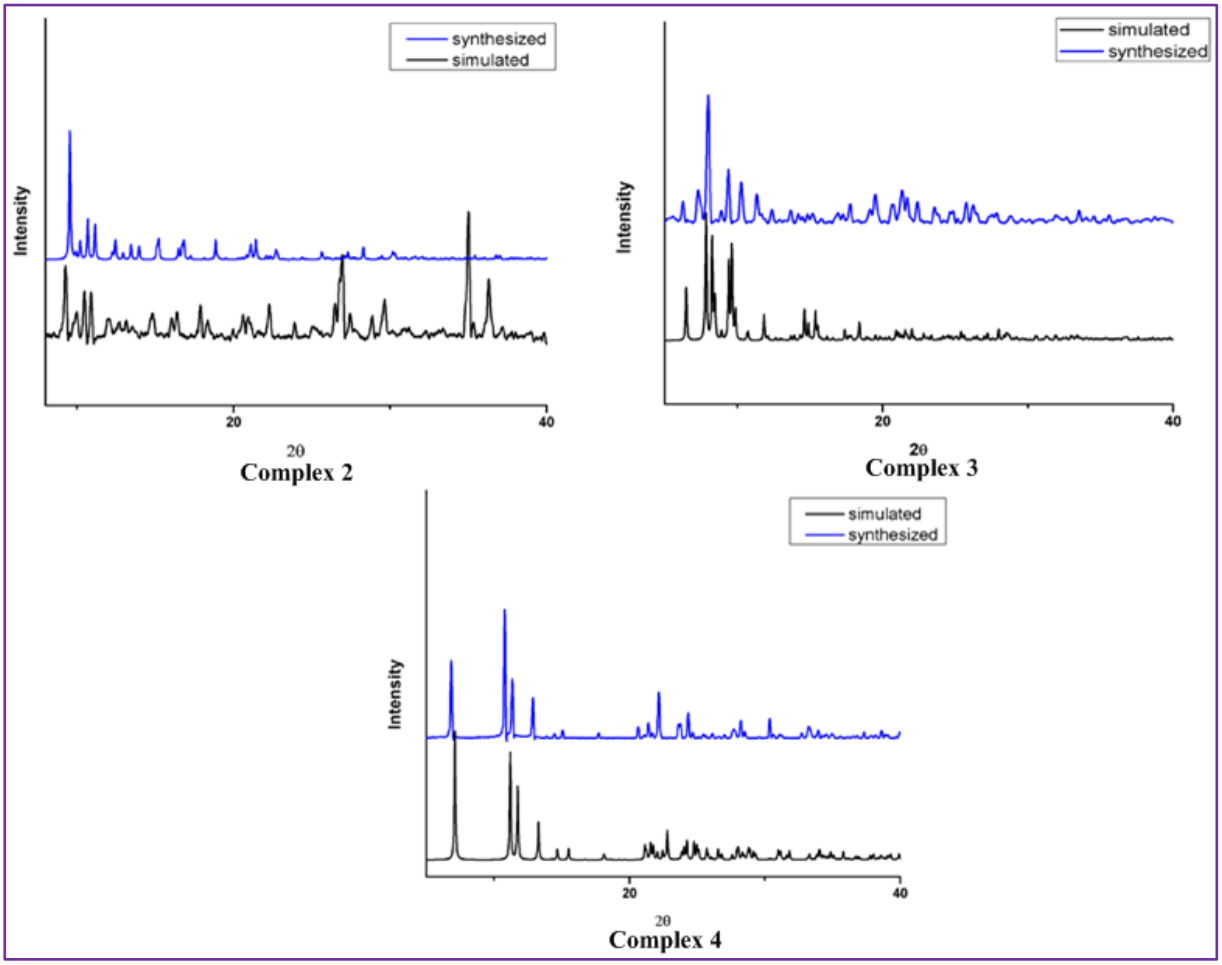

Figure 18: Powder XRD pattern for complexes **2, 3, 4.**

Synthesis of metal sulfide particles:

Cadmium-sulfide fine-particles (FPs): On heating the solution of complex **3** at 180 ^{0}C, colorless solution becomes yellow in color which indicates the formation of cadmium-sulfide fine particles (Scheme 3).

Scheme 3:

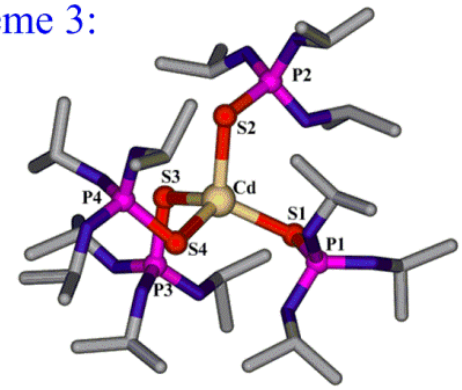

Formamide

170-180 ^{0}C

CdS Fine Particles

Formation of cadmium-sulfide (CdS) FPs was further confirmed by periodic recording of the UV-Visible spectra of the reaction mixture. UV–Vis spectroscopy is used to determine size and shape of fine particles. Figure 19 (a) shows the UV-Visible spectra of cadmium-sulfide FPs. UV-visible absorption spectra of cadmium-sulfide solution contain a single surface plasmon resonance band at 366 nm. The solution of FPs was also monitered under FE-SEM equipped with Energy Dispersive Spectroscopy (EDS). The EDS analysis is shown in Figure 19 (b, c) confirms that the particles are cadmium-sulfide. Atomic weight% of cadmium and sulfur are respectively 50.45 and 49.55, that is 1:1 ratio which indicate formation of CdS fine particles. In these fine particles our ligand $\mathbf{L^1}$ is acting as a capping agent. FE-SEM determination of the dried sample showed formation of cadmium-sulfide FPs (Figure 19 (d, e)). The morphology of the fine particles was found to be spherical and uniform throughout. The cadmium-sulfide particles are nano-sized and in the range of 300-450 nm. We are calling them fine particles because their sizes are more than 100 nm. Fine particle's sizes are found in the range of 100 nm to 2500 nm.

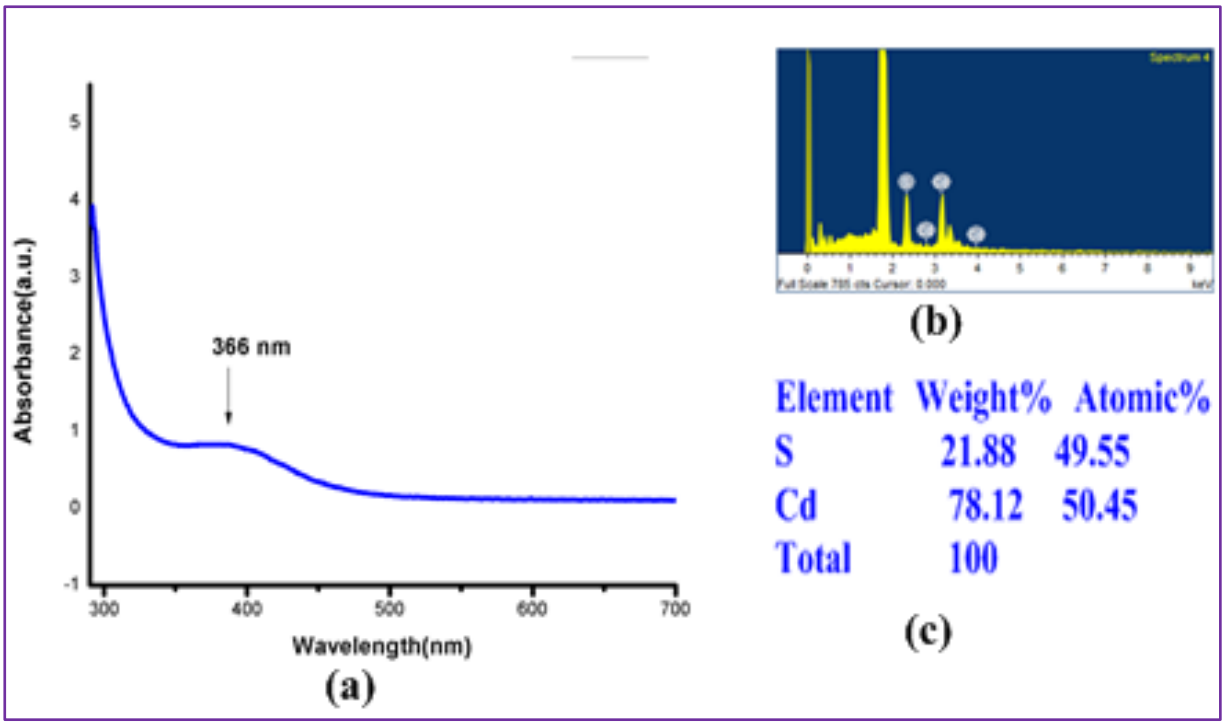

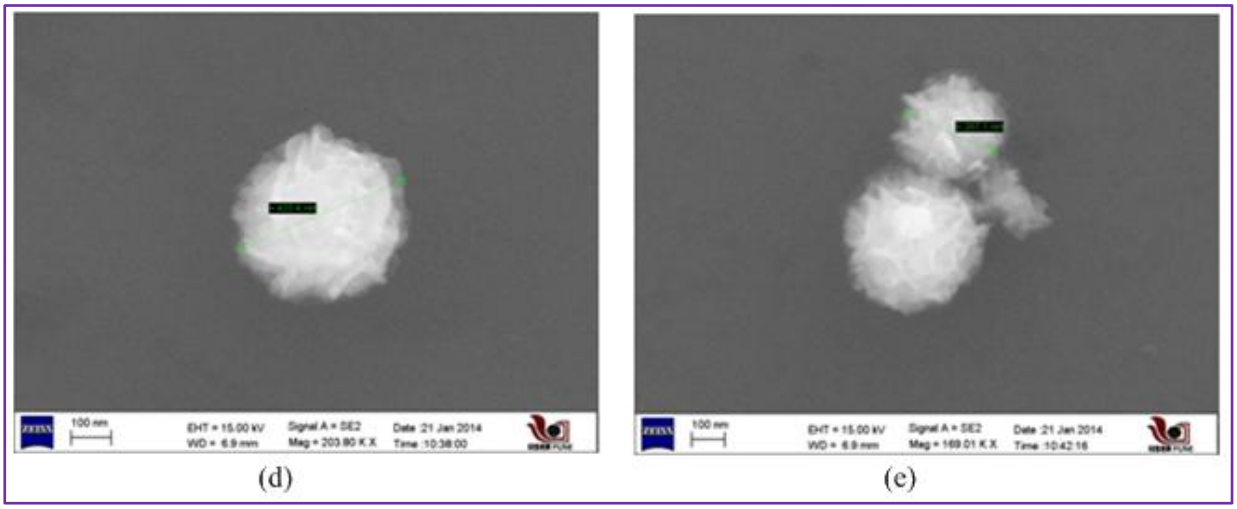

Figure 19: (a) UV visible range spectrum of CdS fine particles showing the surface Plasmon resonance; (b, c) EDS of CdS fine particles; (d, e) SEM images of CdS fine particles.

Silver-sulfide nanoparticles (NPs):

To synthesis Ag_2S NPs, Sodium borohydride ($NaBH_4$) was added to the solution of ligand **L**[1] and $AgNO_3$ (Scheme 2).

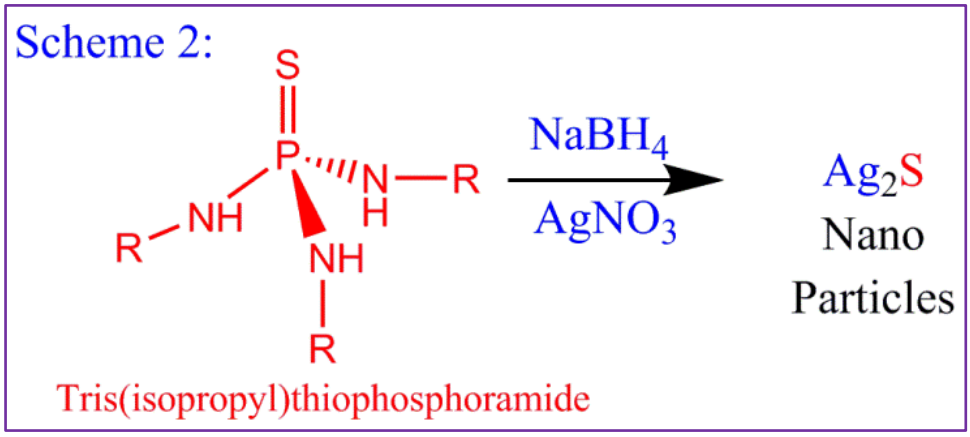

Formation of Silver-sulfide NPs were confirmed by visual inspection of the colour change in solution from colorless to yellow, as well as by periodic recording of the ultraviolet (UV)-vis spectra of the reaction mixture. After adding $NaBH_4$, the colorless mixture of a solution of $AgNO_3$ and **L**[1], changes to yellow which indicates the formation of Ag_2S nano particles. The change in the color of the solution is due to the excitation of surface plasmon vibrations in the NPs, which is characteristic property of the nanoparticles.[20] UV–Vis spectroscopy is used to determine size and shape of these nanoparticles. Figure 20 (a) shows the UV-Visible spectra of silver-sulfide NPs. UV-visible absorption spectra of silver-sulfide solution shows a single surface plasmon resonance band at 445 nm. A broad surface plasmon resonance band is due to aggregation.[21] The morphology and size of NPs thus formed were viewed under FE-SEM equipped with energy dispersive spectroscopy (EDS). The EDS analysis, shown in Figure 20 (b, c), confirms that the particles are Ag_2S. Atomic weight% of silver and sulfur are 66 and 33, respectively. FE-SEM determination of the dried sample showed formation of Silver-sulfide NPs (Figure 20 (e, f, g)). The morphology of the nanoparticles was spherical and uniform. The silver-sulfide particles are nanosized and in the range of 30-40 nm. Figure 20 (d) shows the DLS (Dynamic Light Scattering) profile of silver sulfide NPs which represents its particle size distribution. The average size of the particles is 98.10 nm which is due to dimerization of silver sulfide nano particles.

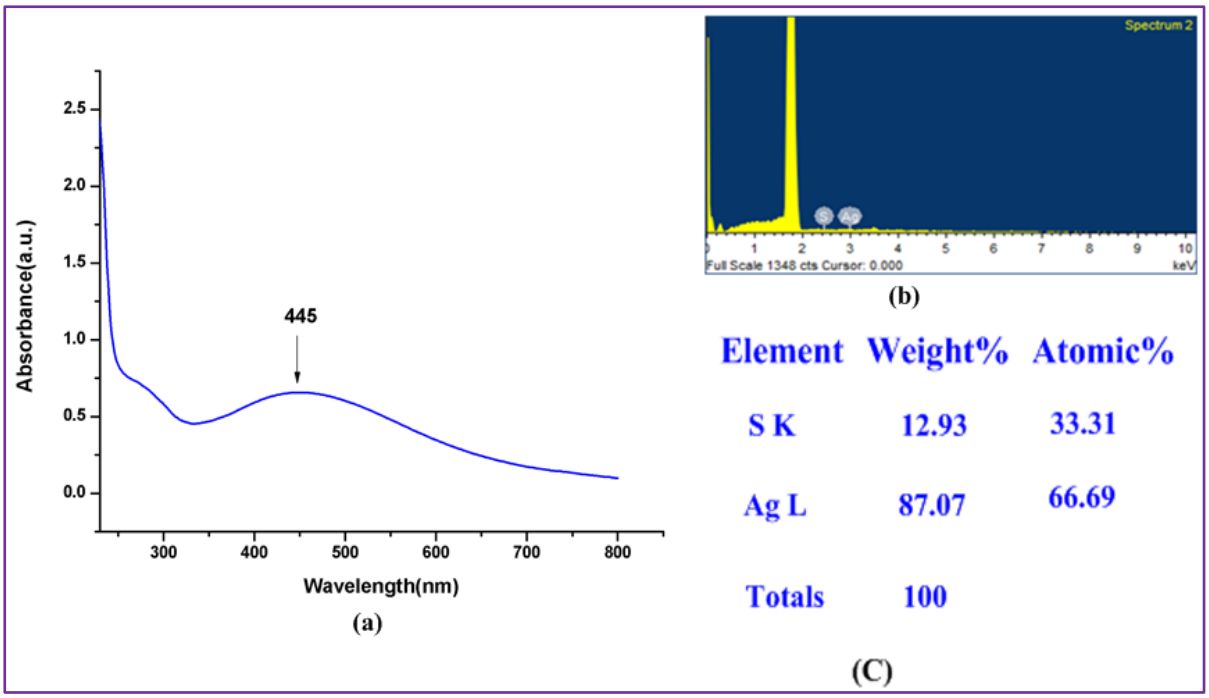

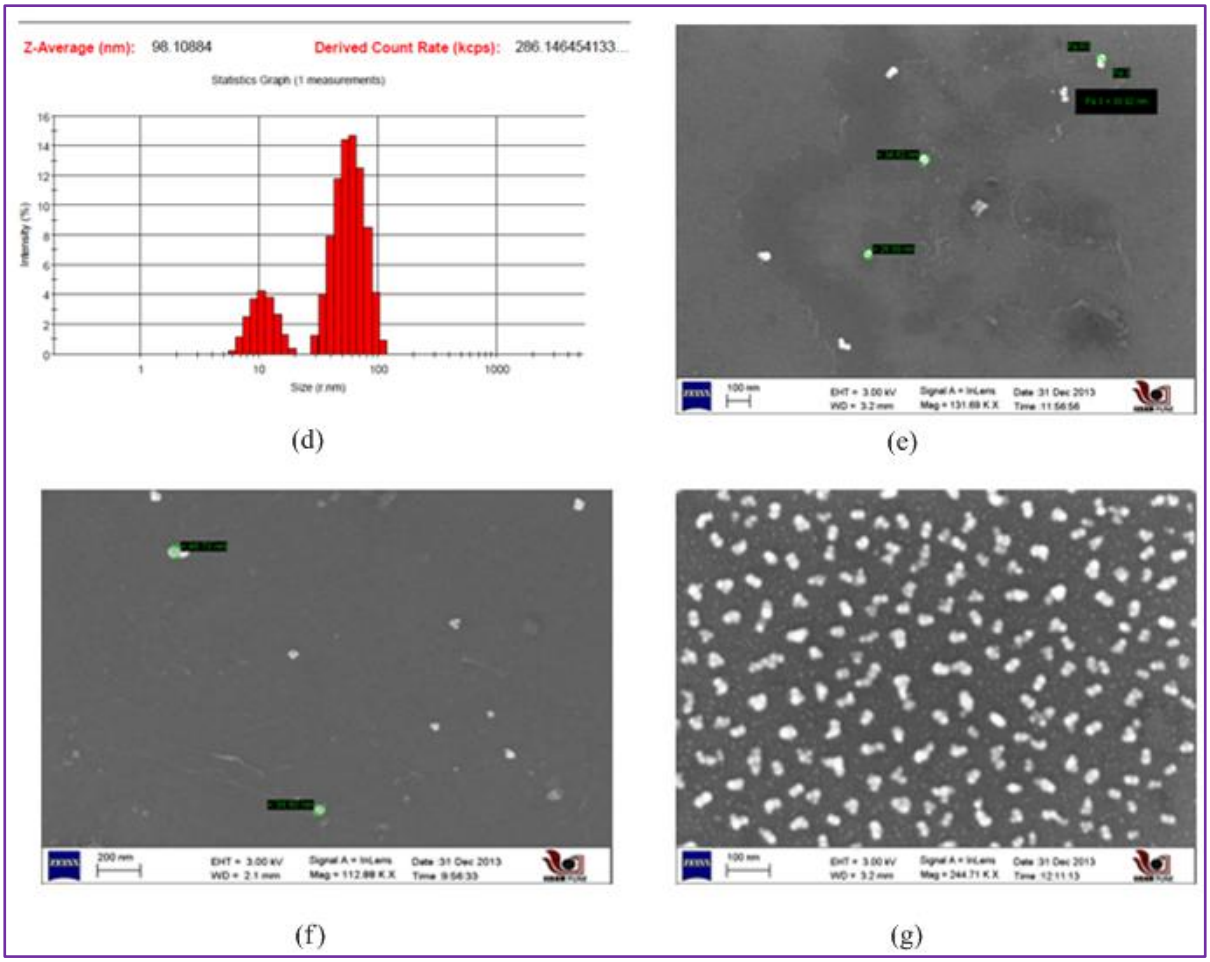

Figure 20: (a) UV visible range spectrum of Ag_2S nano particles showing the surface Plasmon resonance; (b, c) EDS of Ag_2S nanoparticles; (d) DLS of Ag_2S; (e, f, g) SEM images of Ag_2S NPs.

Section II: *Synthesis and Reactivity studies of the Bis(3-Pyridyl)t-butylphosphoramide, [^{t}BuPO(NH^{3}Py)$_3$], ligand (**L^2**).*

Synthesis:

The tert-butylphosphonic dichloride was synthesized as per the reported procedure.[22] The t-butyl phosphoramide ligand **L^2** was synthesized from the corresponding t-butyl phosphoric dichloride ^{t}BuPOCl$_2$ as shown in Scheme **4**. The ^{1}H NMR peaks represent the ligand **L^2** (Figure 21). The ^{31}P-NMR of **L^2** gave a sharp peak at δ 31.78 (Figure 22). The high-resolution ESI-MS spectrum of **L^2** gave a peak at m/z = 291.1374 for the parent ion (Figure 23). The solid-state structure of the ligand was confirmed by SC-XRD analysis (Figure 25).

Scheme 4:

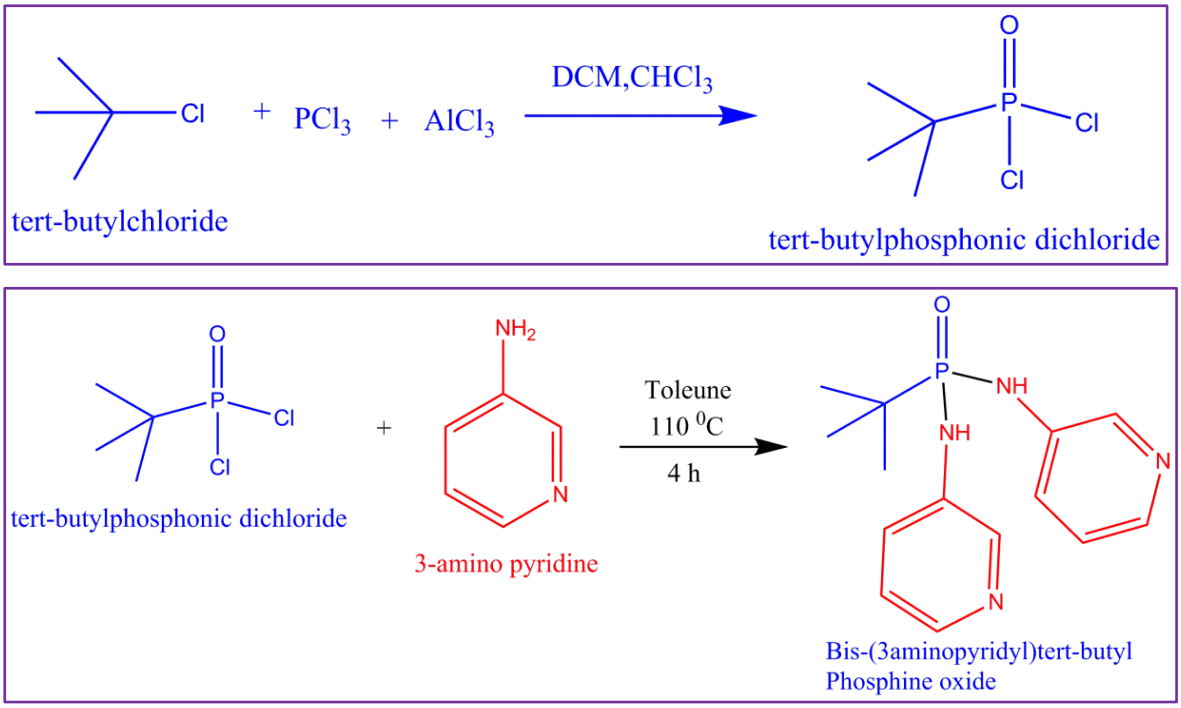

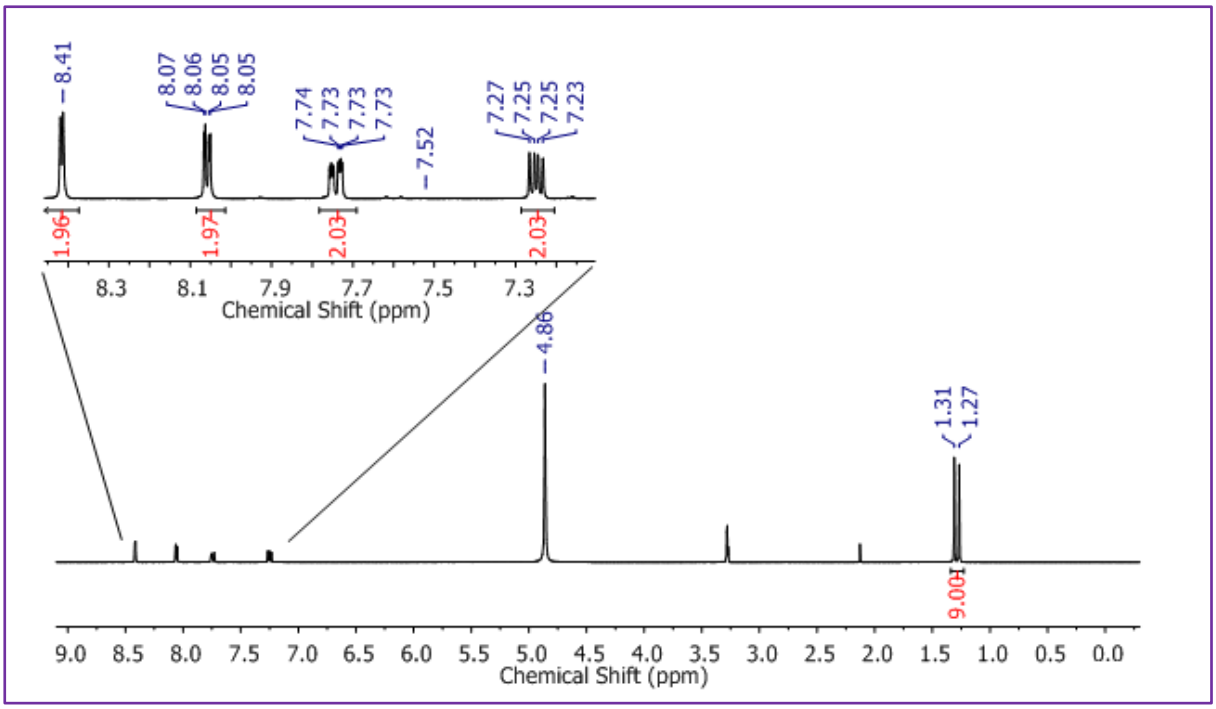

Figure 21: ^{1}H NMR of Bis-(3-aminopyridyl)tert-butyl phosphine oxide **L^{2}**.

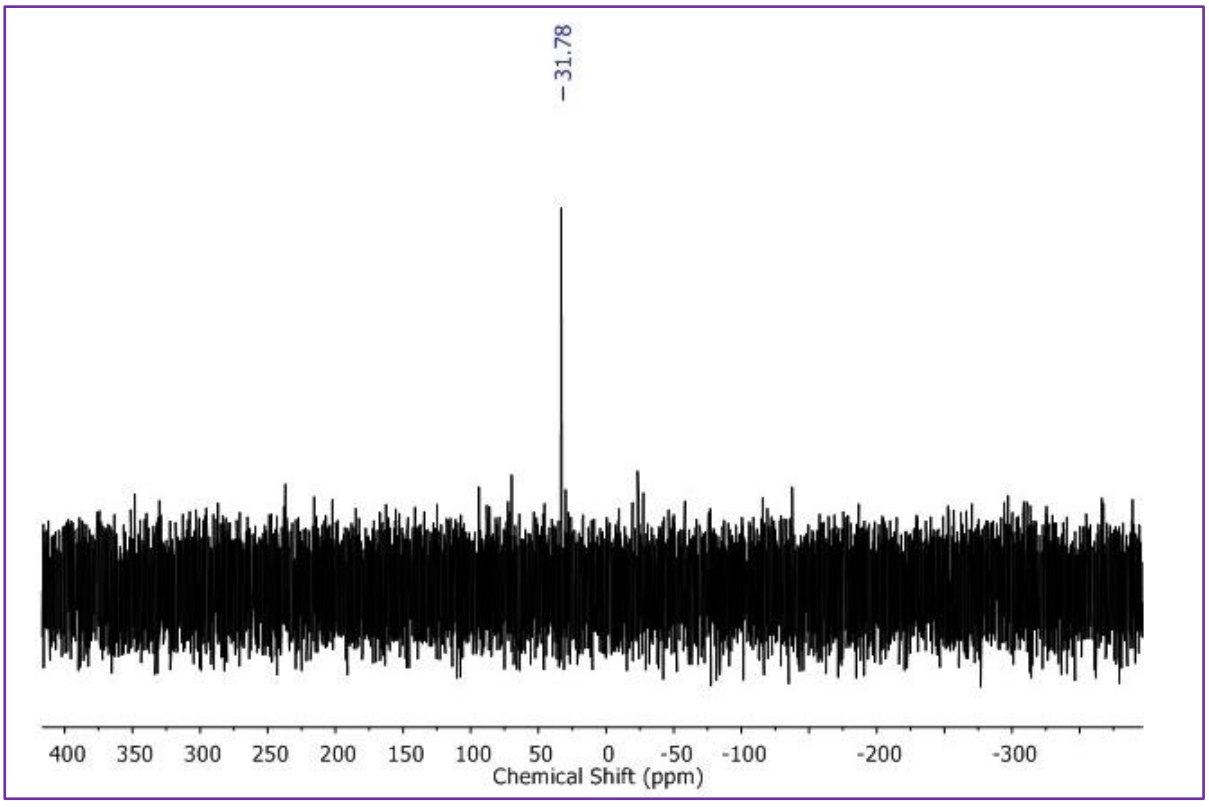

Figure 22: ^{31}P NMR of Bis-(3-aminopyridyl)tert-butyl phosphine oxide **L^{2}**.

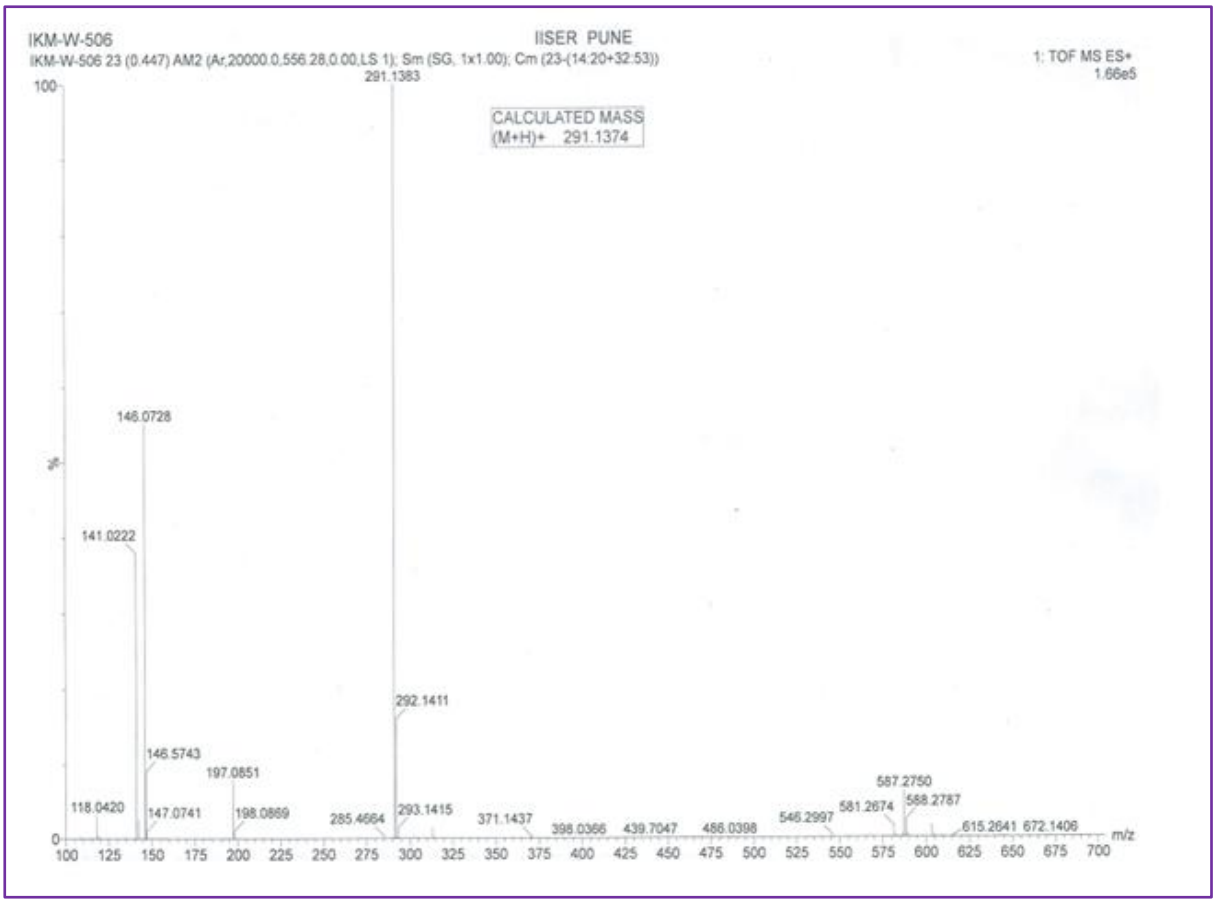

Figure 23: HRMS of Bis-(3-aminopyridyl)tert-butyl Phosphine oxide $\mathbf{L^2}$.

Attempts to deprotonate this ligand with Ag(I) and Pd(II) salts did not lead to any success. Further, the coordination chemistry of this flexible ligand was established with Cu(II) and Ni(II) ions. The ligand $\mathbf{L^2}$ is flexible due to the orientation of its pyridyl rings can be switched to various conformations such as *syn*, *anti* or *in between the two* with respect to the pivotal P=O bond. Thus the reaction of $\mathbf{L^2}$ with $Cu(ClO_4)_2$ gave a cationic 2D-coordination polymer of composition $\{Cu_2[(\mathbf{L^2})_2]_4.4ClO_4\}_n$ assisted by the pyridyl coordination of the ligand. The perchlorate ions provide the necessary charge balance and remain uncoordinated. Performing this reaction with a different Cu(II) source such as $Cu(NO_3)_2$ gave a slightly different network of composition $\{Cu_2[(\mathbf{L^2})_2].2NO_3.2H_2O\}_n$. In this assembly the interaction of the $\mathbf{L^2}$ with Cu(II) ion primarily generates a 1D-assembly which is further linked by the bridging interaction of one of the nitrate ion to give rise to a 2D-network. The other nitrate ion uncoordinated and is located inside the packing cavity. Repeating the reaction in presence of excess of tetra-butyl ammonium nitrate gave only a 1D-network and the nitrate ions remain un-coordinated in the polymer $\{Cu[(\mathbf{L^2})_2]_2.2NO_3.2H_2O\}_n$. However, upon the reaction with a Ni(II) salt, $Ni(NO_3)_2$, $\mathbf{L^2}$ leads to the formation of discrete a tri-nuclear cage assembly of

composition $[Ni_3\mathbf{L}^{\mathbf{2}}{}_6]^{6+}$. Although the exact reason for the formation these subtly different assemblies in **5-8** could not predicted, the flexible nature of ligand and the role of counter ions largely plays a crucial role in these self-assembly reactions. Further, the existence of the Complex **8** was also confirmed with MALDI-TOF which gave a prominent peak at *m/*z 322 corresponding to the species $[M^+/6]$ confirming the hexa-cationic nature of the cage (Figure 24).

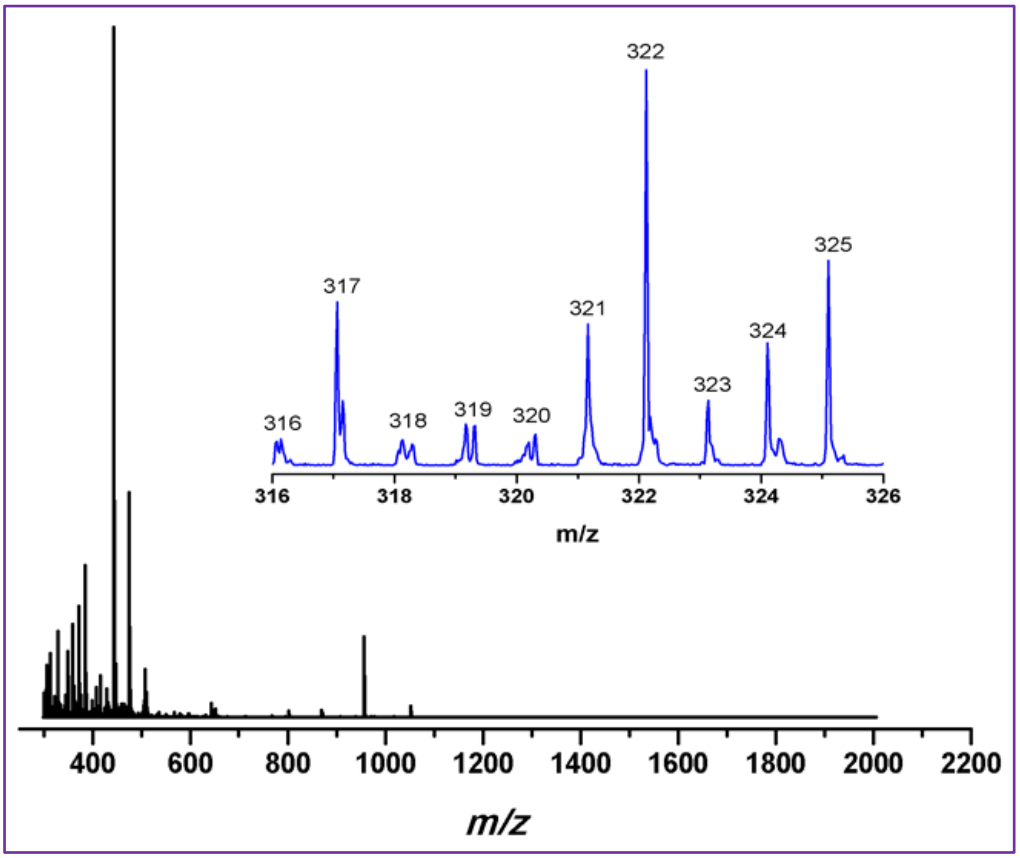

Figure 24: MALDI-TOF Mass spectra of **8** $(M/6)^+$: *m/z* 322.

Crystal Structures:

$C_{14}H_{19}N_4OP$ [L^2]: Ligand L^2 crystallizes in the monoclinic space group $P2_1$. P-N bond distance is 1.66 Å, while the P-O bond distance is 1.494 Å. P-C bond distance is 1.838 Å. Figure 25 (b) shows Hydrogen bonding in ligand L^2.

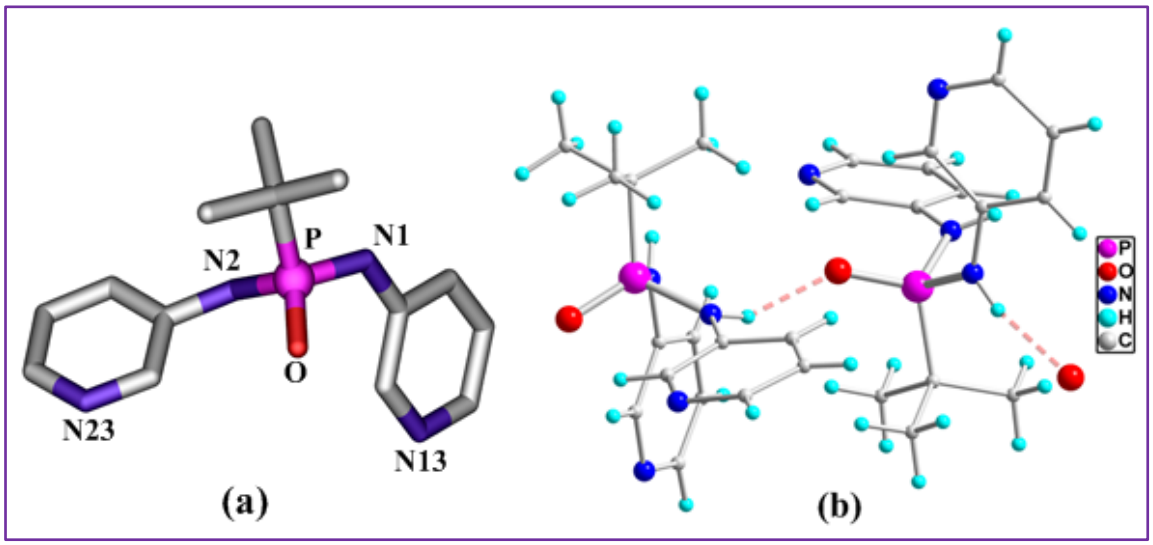

Figure 25: (a) Crystal structure of L^2; (b) Hydrogen bonding in ligand L^2.

$\{Cu_2[(L^2)_2]_4.4ClO_4\}_n$ [5]: The complex **5** was crystallized in the monoclinic space group $P2_1$. The asymmetric unit consists of two Cu(II) ions, four L^2 moieties and four perchlorate anions (Figure 26), where two Cu(II) ions and two ligand moieties construct a macrocycle with the other two ligands acting as a connector/bridge between two such macrocycles. This leads to formation of a 2D sheet structure in space, having two kinds of macrocycles. One is smaller which is explained above, while the other bigger macrocycle (consisting of six Cu(II) ions and six ligand moieties) was constructed using smaller macrocycles and the connector ligands. Each Cu(II) center is bonded to four $N_{pyridyl}$ atoms and one oxygen atom of the coordinated water, giving a square pyramidal geometry around the metal center. Cu-$N_{Pyridyl}$ distances were found in the range of 2.039 Å -2.119 Å, while the Cu-O_{Water} distance was 2.137 Å.

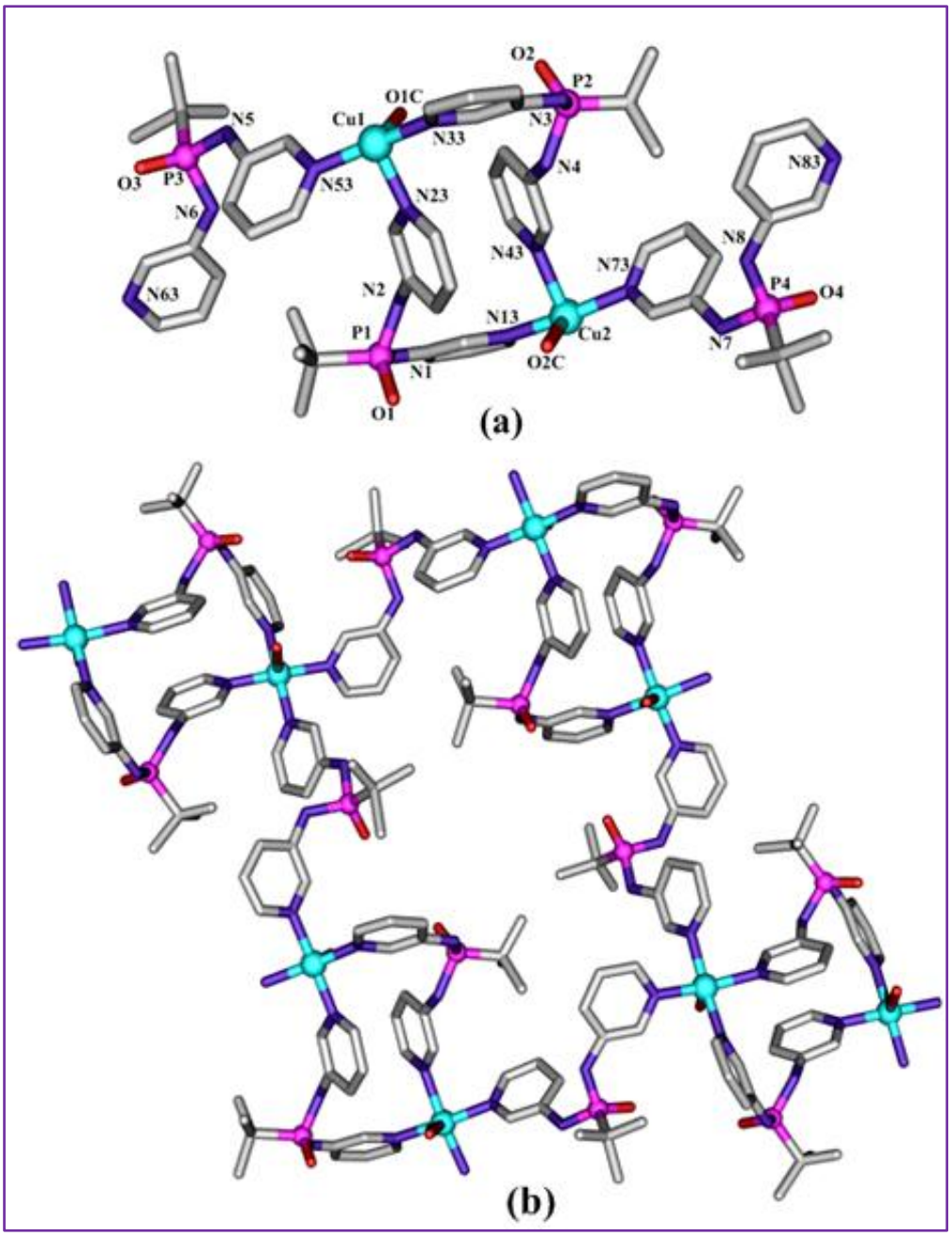

Figure 26: (a) Asymmetric unit (b) 2D polymeric sheet of complex **5.**

$Cu_2[(L^2)_2].2NO_3.2H_2O$ [6]: The 2D-Polymeric sheet **6** was crystallized in the triclinic space group P-1. The asymmetric unit of **6** consist of two Cu(II) ions, one ligand $\mathbf{L^2}$, two nitrate ions and two water molecules (Figure 27). The molecular structure of **6** consist of octahedral Cu(II) atom. The Cu(II) ion is bonded to two $N_{pyridyl}$, two $O_{nitrate}$ and two oxygen atom of the coordinated water. Cu(II)-$N_{Pyridyl}$ bond distance is 2.004 Å. The Cu(II)-$O_{nitrate}$ bond distance is 2.664 Å. Cu(II)-O_{water} bond distance shifted to 1.989 Å.

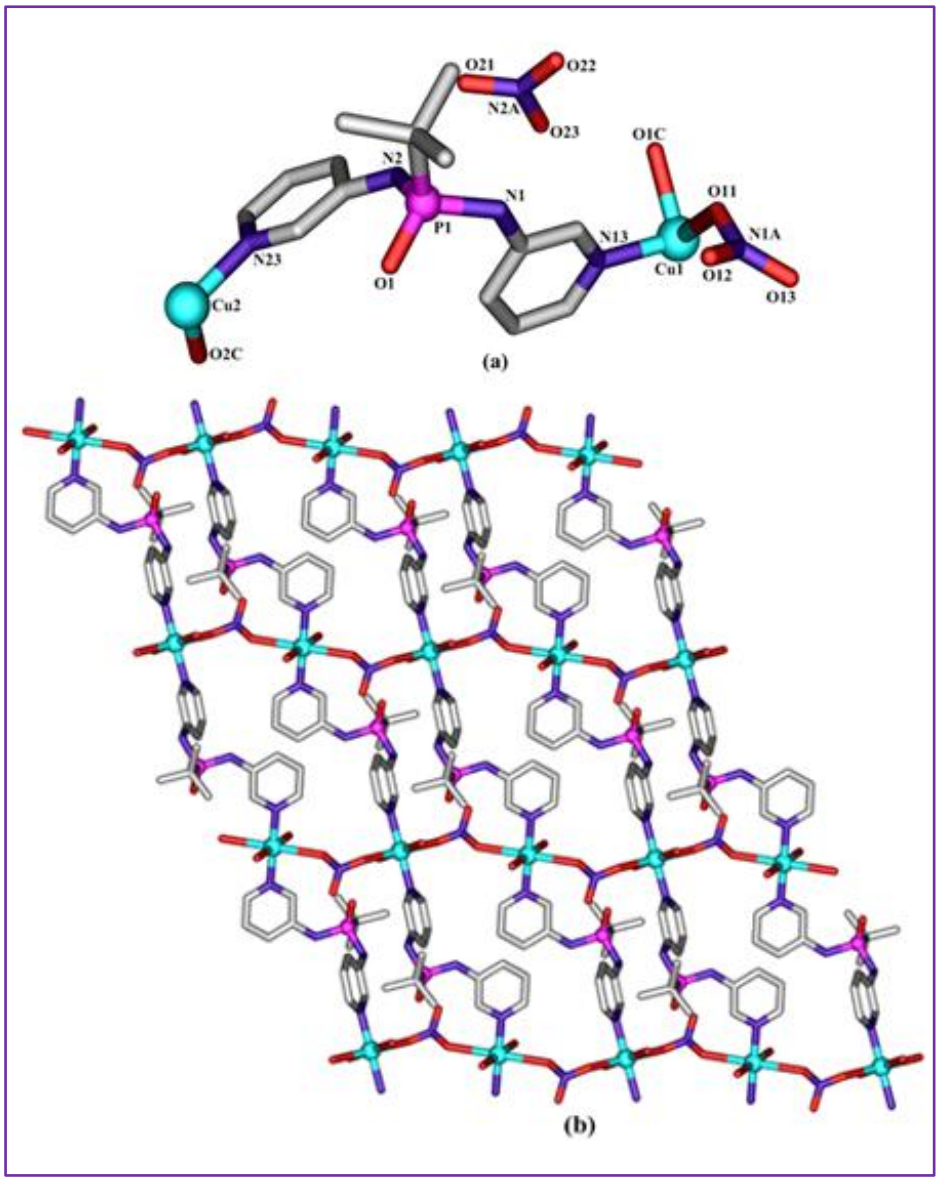

Figure 27: (a) Asymmetric unit (b) 2D polymeric sheet view of complex **6**.

The formation of the 2D-assembly in **6** can be viewed as follows. First the ligand $\mathbf{L^2}$ is acting as a bridge between two Cu(II) ions and lead to the formation of a 1D-sheet assembly. These assemblies are further linked by the μ^2-bridging interaction of one of the nitrate ion completing the 2D-assembly (Figure 27 (b)).

$Cu[(L^2)_2]_2.2NO_3.2H_2O$ [7]: 1D Polymeric zig-zag chain **7** crystallized in the triclinic space group P-1. The asymmetric unit of **7** consist of one Cu(II) ion, two ligand $\mathbf{L^2}$, two nitrate ions and two water molecules (Figure 28). The molecular structure of **7** consist of octahedral Cu(II) atom. The Cu(II) is bonded to four $N_{pyridyl}$ atoms and two oxygen atoms of water

molecules. The Cu(II)-$N_{pyridyl}$ bond distances are found in the range of 2.029 Å -2.077 Å. Cu(II)-O_{water} bond distances are found in the range of 2.293 Å -2.342 Å.

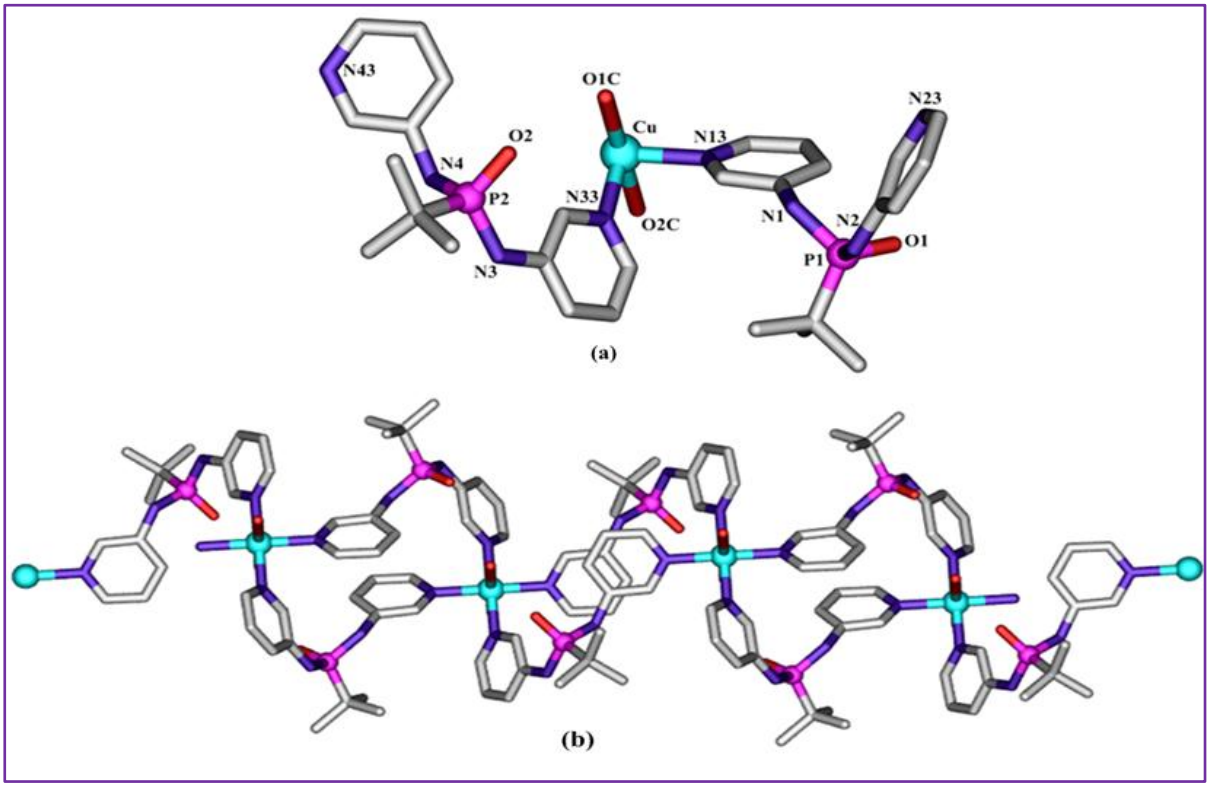

Figure 28: (a) Asymmetric unit (b) 1D Polymeric chain view of complex **7.**

It is interesting to compare the metal-ligand assemblies **5-7.** While the compounds **5** and **7** form 1:2 metal ligand assemblies, **6** forms a 2:1 assembly. Thus, due to the lower availability of the pyridyl N-donor coordination, the metal ion was forced to take up the coordination from the nitrate ion leading to the formation of the anion driven coordination assembly. Further, comparing the orientation of the pyridyl ligand arms in **5**, **6** and **7** are varied with respect to the P=O bond. Thus in **5**, both the pyridyl arms are in anti orientation where as in **6** and **7** they are having mixed *syn-anti* orientation (one of the pyridyl arm is syn and the other one is anti).

$Ni_3[(L^2)_2]_6$ [8]: The molecular structure of the trinuclear cage assembly of **8** was solved in the monoclinic space group C2. The molecular core consists of six ligands $\mathbf{L^2}$, three Ni(II) ions connected in the form of a macrocyclic cavitand (Figure 29). Due to the poor R-value the bond-lengths and angles were not discussed in this report. Nevertheless, the connectivity patterns of this molecule were firmed established from the molecular structure. Interestingly, both the pyridyl arms in all the ligand units are arranged in a syn orientation with respect to

the P=O group. Thus, one of the coordinated water molecules on the Ni(II) ions and the P=O groups of the ligand are located inside the cavity of the molecule. The MSROLL analysis of the molecule gave a cavity volume of approximately 65 $Å^3$. The host-guest chemistry of this cage molecule is currently under study in our group.

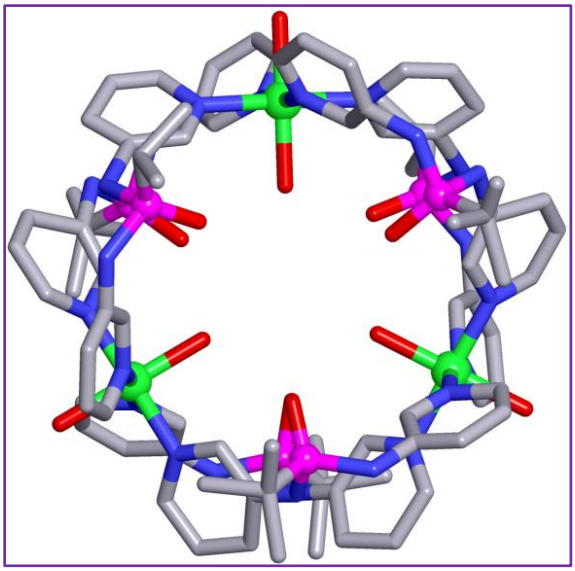

Figure 29: Molecular structure of the Ni(II) complex **8**.

TGA and PXRD for compounds 5, 6, 7, 8:

For understanding the stability of the complex **7, 8** thermogravimetric analysis was performed over a range of temperatures from 30 °C to 546 °C. The Complex **7** shows an initial weight loss of about 12% below 200 °C matching with the removal of two nitrate ions. Above this temperature a rapid weight loss occurs which indicates the decomposition of complex **7.**

The initial 13% weight loss in **8** upto 120 ^oC is due to the loss of coordinated and non-coordinated solvate molecules (water and methanol). The TGA plot in Figure 30 shows the stability of **8** is retained up to a temperature of 250 °C. Above this temperature an abrupt weight loss was observed indicating the decomposition of the complex **8**.

The PXRD pattern of the powdered sample of **5, 6, 7** was found to be exactly matching with the simulated pattern obtained from the crystal structure. This suggests the phase purity and crystallinity of compound **5, 6, 7** is retained in the powder.

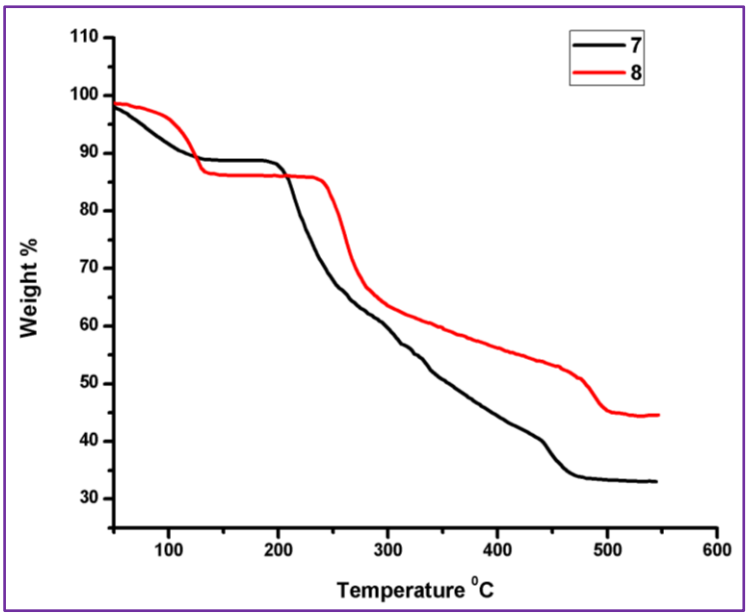

Figure 30: Thermo gravimetric analysis data showing weight loss of complexes **7** and **8**.

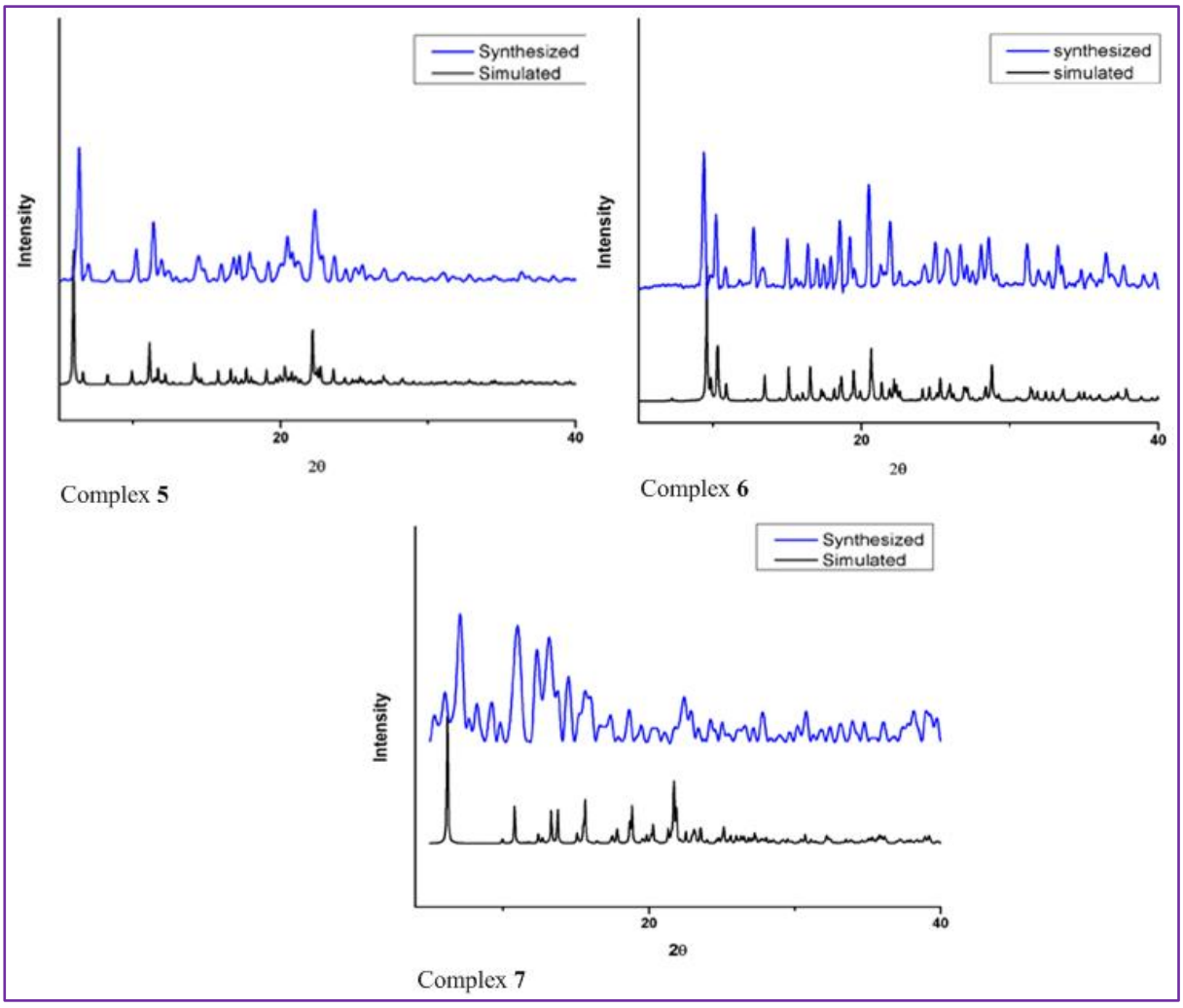

Figure 31: Powder XRD pattern for complexes **5**, **6**, **7.**

Conclusion

In summary, An alkyl functionalized Thio-phosphoramide ligand $\mathbf{L^1}$ was synthesized and its complexes were obtained with Pd(II), Cd(II) and Ag(I) metal ions. A bicapped S-bridged trinuclear complex supported by the thio groups of the ligand was obtained in a direct reaction involving $\mathbf{L^1}$ and Pd(II) salts. One of the three amido arms was found to deprotonate in $\mathbf{L^1}$ when an external base is employed forming a mononuclear Pd(II) complex. Furthermore, the ligand $\mathbf{L^1}$ was used as a capping agent to obtain Ag_2S nanoparticles and CdS fineparticles. In the second part, an alkyl functionalized P(V) phosphoramide ligand $\mathbf{L^2}$ was synthesized and its complexes were obtained with Cu(II) and Ni(II) metal ions. Hierarchical structures in discrete, 1D chain and 2D sheet structures were obtained during these metallation reactions. Functional studies of all the obtained assemblies are currently under study in our laboratory.

Experimental Section

Section I: *Thiophosphoramide, $[SP(NH^iPr)_3]$, ligand and its metal complexes.*

Synthesis of Tris-(isopropyl)thiophosphoramide ligand ($\mathbf{L^1}$) $[SP(NH^iPr)_3]$: Ligand $\mathbf{L^1}$ was synthesized as per the reported prcocedure.[20] Thiophosphoryl chloride (17.89 ml, 29.8 g, 0.176 mol) was added dropwise to an excess of iso-propylamine (90 ml, 62.48 g, 1.057 mol) in diethyl ether (200 ml) at 0 °C. Then the reaction mixture was stirred for 3 h at room temperature. The iso-propylammonium chloride salt formed during the reaction was removed by filtration and it was washed with diethyl ether (200 ml) and toluene (100 ml). The volume of the filtrate was reduced to 70 ml. Then after, hexane (50 ml) was added to it and was kept at -15 °C for 1 day. A white solid formed that contained mostly thiophosphoramide ligand mixed with a small amount of $[^iPrNH(S)P(\mu\text{-}N^iPr)_2P(S)NH^iPr]$. Sublimation of the mixture at 90 °C under vaccum yielded $\mathbf{L^1}$ in pure form (19.97 g, 48%). mp 91-94 °C. Anal. Calcd for $C_9H_{24}N_3PS$: C, 45.54; H, 10.19; N, 17.70. Found: C, 45.40; H, 10.00; N, 17.30. ^{1}H NMR (400 MHz, $CDCl_3$): δ 1.15 (d, 18H, CH_3), 3.46 (septet, 3H, CH). ^{31}P NMR (161 MHz, $CDCl_3$): δ 58.56 (lit. 58.6). IR (cm^{-1}): 3389, 3231 [ν(N-H)]. MS [ESI, *m/z* (rel int.)]: $(M+H)^+$ 238.1506.

Synthesis of $Pd_3[PS(NH^iPr)_3]_6S_2.2ClO_4$ [1]: A solution of $\mathbf{L^1}$ (6 mg, 0.025 mmol) and palladium acetate $Pd(OAc)_2$ (4 mg, 0.17 mmol) in methanol (MeOH) was stirred for 1 h and kept for crystallization. Orange block like crystals suitable for analysis by Single crystal X-ray Diffractometer (SCXRD) were obtained after 6 days. FT-IR data in KBr pellet (cm^{-1}): 3246, 2965, 1630, 1413, 1135 and 1016. Anal. Calcd for $C_{54}H_{144}N_{18}P_6S_8Pd_3Cl_2O_8$: C, 32.33; H, 7.23; N, 12.57. Found: C, 33.97; H, 7.68; N, 12.56.

Synthesis of $Pd[PS(NH^iPr)_2(N^iPr)]_2$ [2]: To the well stirred solution of $\mathbf{L^1}$ (6 mg, 0.025 mmol) and palladium acetate $Pd(OAc)_2$ (4 mg, 0.17 mmol) in methanol, 1 ml aqueous ammonia was added. Then the whole reaction mixture was stirred for 1 h and kept for crystallization at room temperature. Orange block like crystals suitable for analysis by SCXRD were obtained after a week. FT-IR data in KBr pellet (cm^{-1}): 3342, 2963, 2926, 1401, 1201, 1127, 912, 602. MALDI-TOF/TOF: *m/z* 580 (M^+). Anal. Calcd for $C_{18}H_{46}N_6P_2PdS_2$: C, 37.33; H, 8.01; N, 14.51; S, 11.07. Found: C, 37.02; H, 7.89; N, 1486; S, 11.20.

Synthesis of $Cd[PS(NH^iPr)_3]_4$ [3]: To the solution of $\mathbf{L^1}$ (11.2 mg, 0.047 mmol) in methanol, solution of $Cd(ClO_4)_2$ (15.1 mg, 0.048 mmol) in methanol and acetonitrile was added. The resulting colorless solution was stirred for 1 h. After filtering the solution through celite pad, it was kept for crystallization at room temperature. White rods like crystals suitable for SCXRD analysis were obtained within a week. FT-IR data in KBr pellet (cm^{-1}): 3294, 2968, 1412, 1132, 904, 876. MALDI-TOF/TOF: *m/z* 532 $(M/2+H)^+$. Anal. Calcd for $C_{36}H_{96}N_{12}P_4S_4CdCl_2O_8$: C, 34.30; H, 7.68; N, 13.33. Found: C, 34.11; H, 8.01; N, 13.12.

Synthesis of CdS nano particles: Complex **3** (1.06 mg, 0.1 mmol) was dissolved in 10 ml formamide. This solution was heated at 178-180 ^{0}C. After 1-2 h color changes to yellow color which indicates the formation of cadmium-sulfide fine particles. Further it was characterized by UV-Visible spectra, SEM and EDS.

Synthesis of $Ag[PS(NH^iPr)_3].NO_3$ [4]: To a solution of $\mathbf{L^1}$ (11.85 mg, 0.047 mmol) in acetonitrile, a solution of $AgNO_3$ (26 mg, 0.15 mmol) in acetonitrile was added. The resulting mixture was stirred for 1 h and kept at room temperature for crystallization. White crystals suitable for SCXRD analysis were obtained after 25 days. FT-IR data in KBr pellet (cm^{-1}): 3257, 2968, 1382, 1126, 1028. Anal. Calcd for $C_9H_{24}N_3PSAgNO_3$: C, 26.55; H, 5.94; N, 13.76. Found: C, 26.83; H, 6.11; N, 13.88.

Synthesis of Silver-Sulfide nano particles: First solution of starting materials was prepared. $AgNO_3$ (1.6 mg, 1 mmol) was dissolved in 10 ml water. $NaBH_4$ (1.73 mg, 0.046 mmol) was dissolved in 50 ml water. Ligand $\mathbf{L^1}$ (2.3 mg, 1 mmol) was dissolved in 3 ml acetonitrile. Then 1 ml of 0.1M aq. $AgNO_3$ solution and 1 ml of ligand $\mathbf{L^1}$ solution were mixed. Then 400 µl of $NaBH_4$ solution was added. The color of solution changed from colorless to yellow color.

Section II: *Phosphoramide, [^{t}BuPO(NH^{3}Py)$_3$], ligand and its metal complexes.*

Synthesis of Bis-(3aminopyridyl)tert-butyl phosphine oxide (L^2) [OP(t-butyl)(NH^{3}Py)$_2$]: Reported procedure was followed to synthesized the tert-butylphosphonic dichloride. [22] PCl_3 (6.87 ml, 50 mmol, 1equiv.) was added dropwise in the solution of $AlCl_3$ (6.67 g, 50 mmol, 1 equiv) in CH_2Cl_2 (10 ml) and the reaction mixture was stirred for 30 min at room temperature. Pure tert-butylchloride (6.8 ml, 62.5 mmol, 1.25 equiv.) was added and the solution was stirred at room temperature overnight. Then the reaction mixture was diluted with 25 ml of $CHCl_3$ and added to concentrated HCl (15 ml) and 75 g of crushed ice. Aqueous layer was separated and extracted with $CHCl_3$ (10 ml). Organic layers were dried over $MgSO_4$, filtered and concentrated. The crude product was sublimated at 73 ^{0}C to get pure tert-butylphosphonic dichloride. Now tert-butylphosphonic dichloride (2 gm, 11.4 mmol, 1 equiv.) was added to an excess of 3-amino pyridine (7.5 g, 80 mmol, 7 equiv.) toluene (250 ml). The solution was stirred for 4 h at reflux. Crude product was washed with water to get pure compound. mp **275** °C. ^{1}H NMR (CD_3OD, δ): 1.29 (d, 9H, $3CH_3$), 7.23-8.41 (1H, pyridyl CH). ^{31}P NMR (161 MHz, CD_3OD): 31.78 (s). IR (cm^{-1}): 3439, 3120, 1583, 1501, 1474, 1172, 1049, 944, 826. ESI(+): 291.1383 $(M)^+$. Anal. Calcd for $C_{14}H_{19}N_4OP$: C, 57.92; H, 6.60; N, 19.30. Found: C, 57.86; H, 6.12; N, 18.98.

Synthesis of $Cu_2[(L^2)_2]_4.4ClO_4$ [5]: To a solution of $\mathbf{L^2}$ (29 mg, 0.099 mmol) in 2 ml methanol (MeOH), copper perchlorate $Cu(ClO_4)_2$ (18 mg, 0.0486 mmol) in 1 ml water (H_2O) was added. The resulting mixture was stirred for 1 h and kept for crystallization. Blue dot crystals were obtained after 12 days. FT-IR data in KBr pellet (cm^{-1}): 3556, 2963, 2924, 1584, 1478, 1393, 1278, 1086, 931. Anal. Calcd for $C_{56}H_{80}N_{16}O_{22}P_4C_{l4}Cu_2$: C, 39.06; H, 4.68; N, 13.01. Found: C, 38.98; H, 4.62; N, 13.05.

Synthesis of $Cu_2[(L^2)_2].2NO_3.2H_2O$ [6]: To a solution of $\mathbf{L^2}$ (29 mg, 0.099 mmol) in methanol (MeOH), copper nitrate $Cu(NO_3)_2$ (73.8 mg, 0.303 mmol) in water (H_2O) was added. The resulting mixture was then stirred for 1 h and kept for crystallization. Blue crystals were obtained after 10-12 days. FT-IR data in KBr pellet (cm^{-1}): 3515, 3198, 1561, 1224, 1015, 925, 918. Anal. Calcd for $C_{14}H_{23}N_6O_9PCu_2$: C, 29.12; H, 4.01; N, 14.55. Found: C, 29.83; H, 4.11; N, 14.88.

Synthesis of $Cu[(L^2)_2]_2.2NO_3.2H_2O$ [7]: To a solution of $\mathbf{L^2}$ **(**29 mg, 0.099 mmol) in methanol (MeOH) was added copper nitrate $Cu(NO_3)_2$ (12.1 mg, 0.050 mmol) in water (H_2O). Then tetrabutyl ammonium nitrate (TBN) (50 mg, 0.164 mmol) was added in the reaction mixture. The resulting mixture was stirred for 1 h and kept for crystallization. Blue square crystals were obtained after 10-12 days. FT-IR data in KBr pellet (cm^{-1}): 3453, 3203, 2961, 2873, 1583, 1482, 1384, 930, 826, 810. Anal. Calcd for $C_{28}H_{42}N_{10}O_{10}P_2Cu$: C, 41.82; H, 5.26; N, 17.42. Found: C, 24.83; H, 4.11; N, 5.88.

Synthesis of $Ni_3[(L^2)_2]_6$ [8]: To a solution of $\mathbf{L^2}$ (29 mg, 0.099 mmol) in methanol (MeOH), $Ni(NO_3)_2$ (16.8 mg, 0.057 mmol) in water (H_2O) was added. The resulting mixture was stirred for 1 h and kept for crystallization. Blue crystals were obtained after 10-12 days. FT-IR data in KBr pellet (cm^{-1}): 3425, 1473, 1384, 1189, 1059, 931. MALDI-TOF/TOF: *m/z* 322 $(M/6)^+$. Anal. Calcd for $C_{84}H_{114}N_{24}O_6P_6Ni_3$: C, 52.60; H, 59.9; N, 17.53. Found: C, 52.13; H, 58.02; N, 17.12.

References:

(1) (a) Chadwick, A. T. Steric effects of phosphorus ligands in organometallic chemistry and homogeneous catalysis. *Chemical Reviews*. **1977**, *77*, 3. (b) Boomishankar, R.; Richards, P.I.; Gupta, A.K.; Steiner, A. Magnesium and Titanium Complexes of Polyanionic Phosphazenate Ligands. *Organometallics.* **2010**, *29*, 2515–2520

(2) (*a*) Raithby, P. R.; Russell, C. A.; Steiner, A.; Wright, D. S. A. Tetrakis(imido) Phosphate Anion Isoelectronic with PO_4^{3-}. *Angew. Chem., Int. Ed. Engl.* **1997**, *36*, 649; (*b*) Burke, L. T.; Freire, E. H.; Holland, R.; Jeffery, J. C.; Leedham, A. P.; Russell, C. A.; Steiner, A.; Zagorski, A. Synthesis and structure of a tris imido phosphonate anion; the missing link in imido analogues of phosphorus oxoanions *Chem. Commun.* **2000**, 1769.

(3) Buchard, A.; Auffrant, A.; Klemps, C.; Vu-Do, L.; Boubekeur, L.; Le Goff, X. F.; Le Floch, P. Highly efficient P–N nickel(II) complexes for the dimerisation of ethylene. *Chem. Commun.* **2007**, 1502; (b) Sauthier, M.; Fornié-Cámer, J.; Toupet, L.; Réau, R. Palladium(II) Complexes of Chiral 1,2-Diiminophosphoranes: Synthesis, Structural Characterization, and Catalytic Activity for the Allylic Alkylation *Organometallics*. **2000**, *19*, 553.

(4) (a) Zhang, C.; Sun, W.-H.; Wang, Z.-X. Cobalt and Nickel Complexes Bearing Pyrazolyliminophosphorane Ligands: Synthesis, Characterisation and Catalytic Ethylene Oligomerisation Behaviour. *Eur. J. Inorg. Chem*. **2006**, 4895; (b) Masuda, J. D.; Wei, P.; Stephan, D. W. Nickel and palladium phosphinimine-imine ligand complexes. *Dalton Trans*. **2003**, 3500; (c) Alhomaidan, O.; Beddie, C.; Bai, G.; Stephan, D. W. Titanium complexes of amido phosphinimide ligands. *Dalton Trans.* **2009**, 1991. (d) Yadav, K.; McCahill, J. S. J.; Bai, G.; Stephan, D. W. Phosphinimide complexes with pendant hemilabile donors: synthesis, structure and ethylenepolymerization activity. *Dalton Trans.* **2009**, 1636; (e) LePichon, L.; Stephan, D. W.; Gao, X.; Wang, Q. Iron Phosphinimide and Phosphinimine Complexes: Catalyst Precursors for Ethylene Polymerization. *Organometallics*, **2002**, *21*, 1362; (f) Alhomaidan, O.; Bai, G.; Stephan, D. W. Use of Olefin Metathesis to Link Phosphinimide−Cyclopentadienyl Ligand Complexes: Synthesis, Structure, and Ethylene Polymerization Activity. *Organometallics*, **2008**, *27*, 6343.

(5) (a) Buchard, A.; Platel, R. H.; Auffrant, A.; Le Goff, X. F.; Le Floch, P.; Williams, C. K. Iminophosphorane Neodymium(III) Complexes As Efficient Initiators for Lactide Polymerization *Organometallics*. **2010**, *29*, 2892; (b) Sun, H.; Ritch, J. S.; Hayes, P. G. Toward Stereoselective Lactide Polymerization Catalysts: Cationic Zinc Complexes Supported by a Chiral Phosphinimine Scaffold. *Inorg. Chem*. **2011**, *50*, 8063; (c) Rastätter, M.; Zulys, A.; Roesky, P. W. A bis(phosphinimino)methanide lanthanum amide as catalyst for the hydroamination/ cyclisation, hydrosilylation and sequential hydroamination/hydrosilylation catalysis. *Chem. Commun*. **2006**, 874.

(6) (a) Rastätter, M.; Zulys, A.; Roesky, P. W. Bis(phosphinimino)methanide Rare Earth Amides: Synthesis, Structure, and Catalysis of Hydroamination/Cyclization, Hydrosilylation, and Sequential Hydroamination/Hydrosilylation. *Chem.–Eur. J*. **2007**, *13*, 3606; (b) Panda, T. K.; Zulys, A.; Gamer, M. T.; Roesky, P. W. Cyclooctatetraene Complexes of Yttrium and the Lanthanides with Bis (phosphinimino) methanides: Synthesis, Structure, and Hydroamination/Cyclization Catalysis. *Organometallics*. **2005**, *24*, 2197.

(7) (a) Buchard, A.; Heuclin, H.; Auffrant, A.; Le Goff, X. F.; Floch, P. Le. Coordination of tetradentate X_2N_2 (X = P, S, O) ligands to iron(II) metal center and catalytic application in the transfer hydrogenation of ketones. *Dalton Trans*. **2009**, 1659; (b) Cadierno, V.; Díez, J.; García-Álvarez, J.; Gimeno, J. Iminophosphorane-Based Nucleophilic Ruthenium(II) Carbene Complexes: Unusual C-C Coupling and C-H Activation Promoted by the Addition of Alkynes to the Ru=C Bond. *Organometallics*. **2005**, *24*, 2801.

(8) Armstrong, A.; Chivers, T.; Parvez, M.; Boeré, R. T. Stable Cubic Phosphorus-Containing Radicals. *Angew. Chem., Int. Ed.* **2004**, *43*, 502.

(9) Raithby, P. R.; Russell, C. A.; Steiner, A.; Wright, D. S. A. Tetrakis(imido) Phosphate Anion Isoelectronic with PO_4^{3-}. *Angew. Chem., Int. Ed. Engl*. **1997**, *36*, 649−650.

(10) Bickley, J. F.; Copsey, M.C.; Jeffery, J.C.; Leedham, A.P.; Russell, C.A.; Stalke , D.; Steiner, A.; Stey, T. and Zacchini, S. From the tetra(amino) phosphonium cation, $[P(NHPh)_4]$, to the tetra(imino) phosphate trianion, $[P(NPh)_4]^{3-}$, two-faced ligands that bind anions and cations. *Dalton Trans*. **2004**, 989 – 995.

(11) Chivers, T.; Fu, Z.; Thompson, L. K. Structure and magnetic properties of a novel copper halide framework $\{[^{t}BuNH_3]_2[Cu_3(\mu_3\text{-}OH)(\mu_2\ H_2O)Cl_7]\}_n$ synthesized *via in situ* templation. *Chem. Commun*. **2005**, 2339−2341.

(12) Gupta, A. K.; Steinerb, A.; Boomishankar, R. Tri-, hepta- and octa-nuclear Ag(I) complexes derived from 2-pyridyl-functionalized tris(amido)phosphate ligand. *Dalton Trans.,* **2012**, *41*, 9753–9759.

(13) (a) Gupta, A. K.; Nicholls, J.; Debnath, S.; Rosbottom, I.; Steiner, A.; Boomishankar, R. Organoamino Phosphonium Cations as Building Blocks for Hierarchical Supramolecular Assemblies. *Cryst. Growth Des*. **2011**, *11*, 555.

(14) (a) Holman, K.T.; Pivovar, A.M.; Swift, J.A.; Ward, M.D. Metric Engineering of Soft Molecular Host Frameworks. *Acc. Chem. Res.* **2001**, *34*, 107; (b) Schmuck, C.; Wienand, W. Highly Stable Self-Assembly in Water: Ion Pair Driven Dimerization of a Guanidiniocarbonyl Pyrrole Carboxylate Zwitterion. *J. Am. Chem. Soc.* **2003**, *125*, 452;

(15) Gupta, A. K.; Chipem, F. A. S. and Boomishankar, R. A 2-pyridyl(py) attached phosphine imine $[P(Npy)(NHpy)_3]$ and an imido phosphinate ion $[P(Npy)_2(NHpy)_2]^-$ in its Ag(I) complex**.**. *Dalton Trans.* **2012**, *41*, 1848–1853.

(16) (a) Lyons, T. W.; Sanford, M. S. Palladium-Catalyzed Ligand-Directed C−H Functionalization Reactions. *Chem. Rev.* **2010**, *110*, 1147− 1169.

(17) Gupta, A. K.; Boomishankar, R. Unpublished results.

(18) Gupta, A. K.; Reddy, S. A. D.; Boomishankar, R. Facile Formation of Stable Tris(imido)phosphate Trianions as Their Tri- and Hexanuclear Pd(II) Complexes in Protic Solvents. *Inorg. Chem.* **2013**, *52*, 7608−7614.

(19) Chivers, T.; Krahn, M.; Schatte, G.; Parvez, Masood. Lithiation of Tris(alkyl- and arylamido)orthophosphates $EP[N(H)R]_3$ (E = O, S, Se): Imido Substituent Effects and P=E Bond Cleavage. *Inorganic Chemistry*, **2003**, *42*, 3994.

(20) Nithya, R.; Ragunathan, R. Synthesis of silver nanoparticles using a probiotic microbe and its antibacterial effect against multidrug resistant bacteria. *African Journal of Biotechnology,* **2012**, *11*, 11013.

(21) Hussain, J. I.; Kumar, S.; Hashmi, A. A.; Khan, Z. Silver Nanoparticles: Preparation, Characterization, And Kinetics. *Adv. Mat. Lett*. **2011**, *2*, 188-194.

(22) Slowinski, F.; Aubert, C.; Malacria, M. Diastereoselective Cobalt-Mediated [2+2+2] Cycloadditions of Substituted Linear Enediynes Phosphine Oxides: Scope and Limitations. *J. Org. Chem*. **2003**, *68*, 378-386.